İSTANBUL TECHNICAL UNIVERSITY ★ INSTITUTE OF SCIENCE AND TECHNOLOGY

ANALYSIS OF INVERSE PROBLEMS RELATED TO DIELECTRIC OBJECTS BURIED UNDERGROUND

M. Sc. Thesis by
Ulaş ADİYAN

Department: Electronic and Communication Engineering

Programme: Telecommunication Engineering

JUNE 2010

İSTANBUL TECHNICAL UNIVERSITY ★ INSTITUTE OF SCIENCE AND TECHNOLOGY

ANALYSIS OF INVERSE PROBLEMS RELATED TO DIELECTRIC OBJECTS BURIED UNDERGROUND

M. Sc. Thesis by
Ulaş ADIYAN
(504071337)

Date of submission : 07 May 2010
Date of defence examination: 02 June 2010

Supervisor (Chairman) : Assoc. Prof. Dr. Ali YAPAR (ITU)
Members of the Examining Committee : Prof. Dr. Sedef KENT (ITU)
Prof. Dr. Özcan KALENDERLİ (ITU)

JUNE 2010

İSTANBUL TEKNİK ÜNİVERSİTESİ ★ FEN BİLİMLERİ ENSTİTÜSÜ

YERALTINDA GÖMÜLÜ OLAN DİELEKTRİK CİSİMLERE İLİŞKİN TERS PROBLEMLERİN ANALİZİ

YÜKSEK LİSANS TEZİ
Ulaş ADİYAN
(504071337)

Tezin Enstitüye Verildiği Tarih : 07 Mayıs 2010
Tezin Savunulduğu Tarih : 02 Haziran 2010

Tez Danışmanı : Doç. Dr. Ali YAPAR (İTÜ)
Diğer Jüri Üyeleri: Prof. Dr. Sedef KENT (İTÜ)
Prof. Dr. Özcan KALENDERLİ (İTÜ)

HAZİRAN 2010

FOREWORD

I would like to express my deep appreciation and thanks for my advisor Assoc. Prof. Dr. Ali YAPAR who supports me during this study with his great help and many valuable contributions to this thesis.

May 2010

Ulaş ADİYAN

Telecommunication Engineer

TABLE OF CONTENTS

Page

LIST OF FIGURES

Page

LIST OF SYMBOLS

$\boldsymbol{\mu_0}$: Permeability of the free space
$\boldsymbol{\mu_1}$: Permeability of the upper half space
$\boldsymbol{\mu_2}$: Permeability of the upper half space
$\boldsymbol{\mu_{obj}}$: Permeability of the object
$\boldsymbol{\varepsilon_0}$: Dielectric permittivity of the free space
$\boldsymbol{\varepsilon_1}$: Relative dielectric permittivity of the upper half space
$\boldsymbol{\varepsilon_2}$: Relative dielectric permittivity of the lower half space
$\boldsymbol{\varepsilon_{obj}}$: Relative dielectric permittivity of the object
$\boldsymbol{\sigma_1}$: Conductivity of the upper half space
$\boldsymbol{\sigma_2}$: Conductivity of the lower half space
$\boldsymbol{\sigma_{obj}}$: Conductivity of the object
$\vec{\boldsymbol{E}}$: Electric field vector
$\vec{\boldsymbol{H}}$: Magnetic field vector
$\boldsymbol{k_1}$: Wave number for the upper half space
$\boldsymbol{k_2}$: Wave number for the lower half space
$\boldsymbol{k_{obj}}$: Wave number for the object
$\boldsymbol{w}$: Angular frequency
$\boldsymbol{f}$: Frequency
$\boldsymbol{\lambda}$: Wavelength
$\boldsymbol{G}$: Green's function
$\widehat{\boldsymbol{G}}$: Fourier transform of G
$\boldsymbol{\delta}$: Dirac delta distribution
$\boldsymbol{H_0^{(1)}}$: Zero order Hankel Function of the first kind
$\boldsymbol{u}$: Total field
$\boldsymbol{u_i}$: Incident field
$\boldsymbol{u_s}$: Scattered field
$\boldsymbol{v}$: Object Function
$\boldsymbol{\alpha}$: Scaling parameter in Tikhonov regularization

ANALYSIS OF INVERSE PROBLEMS RELATED TO DIELECTRIC OBJECTS BURIED UNDERGROUND

SUMMARY

In this thesis, some inverse scattering problem are applied for two-dimensional buried objects in two part-space geometry with planar interface. The two-part space mentioned can be considered as two separate parts such as air and soil in the content of this thesis. This makes actually a mathematical problem important in terms of applicability. So, the problem can be adapted to a wide range from buried objects (mines, subsidence, leakage etc. detecting) to the medical applications.

This work takes the inverse scattering problems related to some comparisons as basis. But in order to solve the inverse problem; the data that will be used for inverse problems is needed to be created or measured. So, first of all we solve the forward problem because we will work theoretically. Besides, the solution of the forward problem is very important, since it is used in some applications of the inverse problems. The forward problem will start with the solution of the Green's function in two part space with planarly interface. Then we will handle the non-linearity of the scattering problems by using a numerical method, method of moments, for the solution of the given geometry. Forward problem is solved which make an important contribution to the solution of the inverse problem by the procedure explained. The datas which belongs to the measurement data of the scattered field, acquired from this part. It will be used in the solution of the inverse problem.

Two methods are used in the solution of the inverse problem basically. Firstly, the inverse problem is solved in the sense of Born Method. Born Method depends on a simple approach subject to weak scattering. In this method, the scattering field is ignored in the second kind Fredholm integral equation. After that, some optimizations for Born Method are made in order to increase validation limits and accurate results. These optimizations stand for multi source configuration. In multi-source configuration, it is utilized from the locations of the sources as well as the increased measurement data with the same unknown cell parameters brings better results. However Born Method can not be good enough to give any information for the characteristic of the object. In order to deal with the present disadvantage, Newton Method which is an iterative approach is taken into consideration. Newton Method aims to converge to the true profile's object function by using an initial guess for the object function with a determined iteration number. Also, the mathematical expressions for the Newton Method is determined for the multi-source configuration. The results are discussed in the conclusion part.

Variational numerical applications are done for the methods and approaches given above. Some of the applications are implemented in order to compare the methods and approaches, and to see the validation limits of them. The advantages of the geometry used in this thesis are searched and the approaches can be made for decreasing the computational cost examined.

Important results are found from the numerical applications. For instance; due to the complex approach of Newton Method compared to Born Method, it gives better results for the same configurations. One of the most important results of this work is the remarkable positive effect of the multi-source configuration. Moreover, the locations of the sources for the given geometry bring another important result. However, the approaches used for this geometry showed an important problem; computational cost. Thus, another remarkable result for the problem is that the computational cost can be decreased under some constrains.

YERALTINDA GÖMÜLÜ OLAN DİELEKTRİK CİSİMLERE İLİŞKİN TERS PROBLEMLERİN ANALİZİ

ÖZET

Bu tez çalışmasında, düzgün bir şekilde bölünmüş iki parçalı bir uzayda; iki boyutlu gömülü cisimlerin tespiti için belirli ters saçılma problemleri uygulanmıştır. Bahsedilen iki parçalı uzay bu tez kapsamında hava ve toprak gibi iki ayrı parça olarak düşünülmüştür. Bu da uygulanabilirliği açısından aslında bir matematik problemini önemli bir hale getirmektedir. Buradan hareketle, bu problem gömülü cisim uygulamalarından (maden, göçük, kaçak vs. arama) medikal uygulamalara kadar bir çok alana uyarlanabilir

Bu çalışma ters saçılma problemlerinin çeşitli karşılaştırmalarla çözümlerini esas almıştır. Ancak ters problemin çözülebilmesi için öncelikle ters problemde kullanılacak olan verinin ya oluşturulması ya da ölçülmesi gerekmektedir. Biz teorik bağlamda çalışacağımız için, öncelikle düz problemi çözdük. Düz problemin çözümü, ayrıca ters problemin belirli uygulamalarında kullanıldığından dolayı ekstra bir önem taşımaktadır. Düz problemin çözümü, iki parçalı uzayda Green fonksiyonunun çözümüyle başlamaktadır. Daha sonra belirli bir geometri için sayısal bir yöntem olan momentler yöntemi ile lineer olmayan bir problem lineerleştirilmiştir ve ters problemin çözümüne katkı sağlayacak olan düz problem çözülmüştür. Burada elde edilen saçılan alana ait ölçüm verileri ters problemin çözümünde kullanılmıştır.

Ters problemin çözümünde temel anlamda iki metod kullanılmıştır. İlk olarak Born Metodu kullanılarak problem çözülmüştür. Born Metodu zayıf saçılmalara bağlı olarak basit bir yaklaşıklığa dayanmaktadır. İkinci tür Fredholm integral eşitliğinde saçılan alan ihmal edilmiştir. Bu yöntemin geçerlilik aralığını genişletebilmek ve daha doğru sonuçlar yakalayabilmek için bu metod üzerinde belirli iyileştirmeler yapılmıştır. Bu iyileştirmeler çoklu kaynak yapısına dayanmaktadır. Çoklu kaynak yapısında kaynakların konumundan yararlanıldığı gibi, artan veri sayısıyla aynı sayıda bilinmeyen hücre parametreleri daha iyi sonuçları getirmektedir. Ne var ki; Born Metodu her iki yapı için de cismin karakteristiğine dair önemli bir bilgi vermemektedir. Bu eksikliği gidermek için de iteratif bir yaklaşım olan Newton Metodu ele alınmıştır. Newton Metodu cisim fonksiyonuna dair bir başlangıç değeri belirleyerek; bu değer üzerinden belirli sayıda iterasyonla gerçek cisime ait cisim fonksiyonuna yaklaşmayı hedefler. Newton Metodu için de çoklu kaynak yapısının matematiksel ifadeleri düşünülmüş ve sonuçlar bölümünde tartışılmıştır.

Yukarıda ifade edilen yöntemler ve yaklaşımlar üzerinden çeşitli sayısal uygulamalar yapılmıştır. Sayısal uygulamalardan bazıları yöntem ve yaklaşımları karşılaştırmak ve geçerlilik aralıkları hakkında fikir sahibi olmak için yapılandırılmıştır. Bazı uygulamalarda ise problem geometrisinin getirdiği avantajlar ve hesaplama yükünün azaltılabilmesi için neler yapılabileceği incelenmiştir.

Sayısal uygulamaları göz önünde bulundurarak önemli sonuçlara ulaşılmıştır. Newton Metodu Born Metoduna göre daha ileri bir yaklaşıklığa sahip olduğunda ötürü çok daha iyi sonuçlar üretmiştir. Bu çalışmanın en önemli sonuçlarından biri problemlerin çözümünde kullanılan çoklu kaynak yapısının sonuçları çok önemli bir biçimde değiştirmesidir. Bununla beraber problemin geometrisinde kullanılan kaynak yerleri yansımaya bağlı olarak problem için başka önemli bir sonucu üretmiştir. Ancak bu geometri bu tip problemler için önemli bir sorunu da beraberinde getirmiştir; hesaplama yükü. Bu problem için başka önemli bir sonuç olan, belirli koşullar altında hesaplama yükünün azaltılabileceği sonucuna varılmıştır.

1. INTRODUCTION

Scattering problems constitutes a very important class in electromagnetic theory due to their practical applications in the areas of communications, radar, geophysical exploration, medical imaging, nondestructive testing, military and defence technologies, avionics, space researchs etc. In a general view scattering theory is concerned with the effect of obstacles or inhomogeneities upon some certain incident waves. The scattering problems can be simply classified into two categories; i) direct or forward and ii) inverse scattering problems. The forward problem is concerned with determining the scattered field from the knowledge of the incident field and the obstacle. In the inverse problem the main aim is to determine the characteristics of an object (its shape, location, electromagnetic properties etc.) from measurement data of scattered field. The inverse problems of electromagnetic theory can also be classified into some classes according to the aim of the problem or according to the host medium where the unknown obstacle is placed [1, 2]. Among these classes buried object reconstruction problems are very attractive since not only they have very important applications in the areas such as mine detection, geophysical exploration, mine and petroloum engineering, nondestructive testing etc, but also they are still open to new theoretical investigations as well as experimental contributions. Classical methods such as Born approximations, Newton based methods, contrast source inversion algorithms and some of their modified versions are very well established by many researchers and a huge number of studies can be found in the open literature which we will not give a full list here. Although the basic principles of these methods resembles to each other all of them have its own characteristics according to the problem in hand. According to the geometrical and physical configuration (and also according to the aim) one should choose the most appropriate one in order to reach better images. For this reason the comparison of the

methods for a given configuration will also be a contribution to the theory. The measurement system or configuration is also a very crucial point in the inverse problems related to the buried objects. The reconstruction quality is directly affected by source-receiver configurations (numbers and locations of source and receivers), size of reconstruction domain and properties of background media In this framework, a well known inverse problem related to the dielectric objects buried in a two half space medium will be comparatively analyzed by two different methods (Born approximation and Newton method) and the effects of some parameters mentioned above will be investigated in this study. To this aim the problem is first formulated by a system of integral equations which consists of 2 eqautions known as data and object equations by the aid of the Green's function of two half-spaces. Then this system is solved for different kind of source and receiver configurations by two methods, i.e; Born and Newton methods. Many numerical examples are given in order to show the capabilities of the methods as well as to see the effects of some parameters such as number of sources, frequency, size of reconstruction domain, depths of the buried objects etc. on the solution. In the next subsection the problem will be defined in details.

1.1 Geometry of the Problem

There are various types of source and observer configurations which can be decided with respect to the conception of the pratic problem. For example two part space can be a model for underground and free space which is the configuration related to the problem of this thesis. But the interface will be considered as planar differs from a real model while the problem will be taken in 2-D.(two dimensions) That means, the third dimension is imagined as infinite; which makes the problem as shown in Figure 1.1.

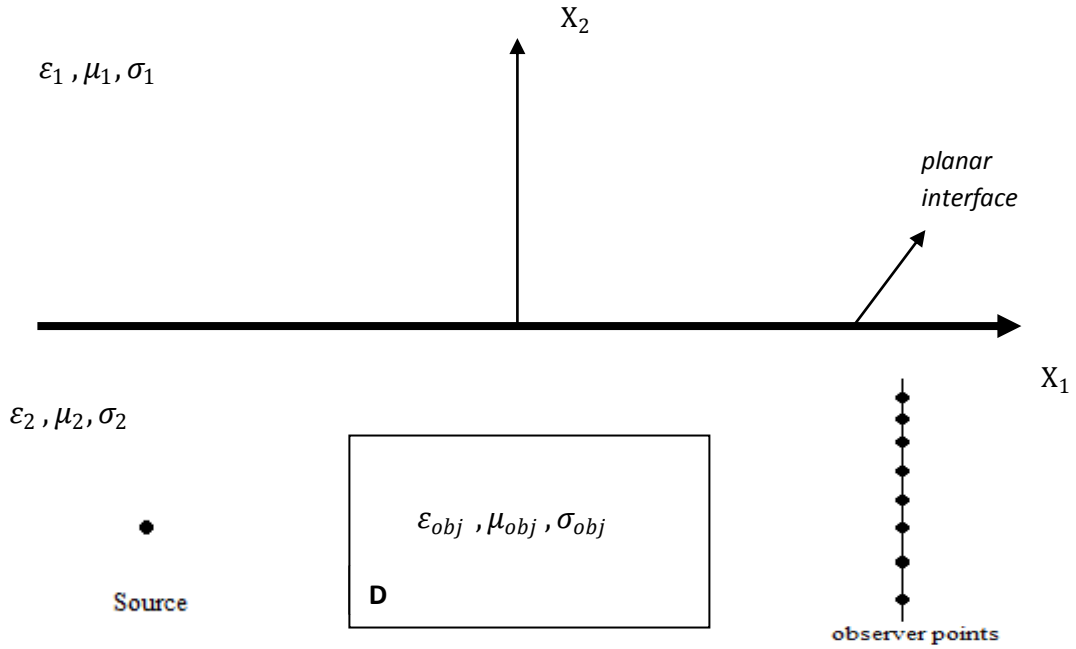

Figure 1.1 : Geometry of the problem

From Figure 1.1 it can be seen that the space is divided to two parts; upper part which has the electromagnetic characteristics $\varepsilon_1, \mu_1, \sigma_1$ are the parameters of the free space while $\varepsilon_2, \mu_2, \sigma_2$ are the parameters of underground. D region where our object is located has the characteristics ε_{obj} , μ_{obj} , σ_{obj} .

Source and observers are chosen for $X_2 < 0$ (in geophysics it is called well to well tomography or cross borehole configuration) , because it can be suggested that this kind of configuration can be a better model for a good imaging compared to source and observer's location $X_2 > 0$.

1.2 Background of the Problem

A. J. Devaney investigated the foundations of diffraction tomography for offset vertical seismic profiling and well to well tomography for weakly inhomogeneous formations which the Born or Rytov approximations for inverse problems can be employed [3].

While Devaney thought the source in the upper part like point source, J. M. Harris presented both theory and numerical simulations of diffraction tomography for arrays of line sources [4]. His work was on propagating fields satisfying the Born and Rytov approximations as Devaney in weakly inhomogeneous media and provides convenient means for treating both forward and inverse scattering problems.

After these basic works, the researchers made valuable improvements in those inverse problems. Some of researches developed the algorithms or numerical implementations for forward problems which made contribution to the general scattering problems. In [5] Richmond advanced the theory and equations for the scattering pattern of a dielectric cylinder of arbitrary cross section shape. He gives almost an exact solution compared to an analytical solution of a dielectric cylinder. He uses a numerical method, by dividing the cylinder into the small cells. While the total scattered field is calculated; a superposition of the cells are used. The research of Richmond has an important role while calculating the measurement scattering data in this thesis which will be detailed in the forward problem section.

Besides; the algorithms for inverse problems, for instance reconstruction problem, are such a good and developing working area that makes these problems very attractive. [6] investigated a new reconstruction problem based on the approximations in [3,4] . They assigned a cost functional as the norm of the difference between the measured scattered field and the calculated one for an estimated object function. Then the inverse scattering problem became as an optimization problem. They minimized the functional and find a new object function for each iteration [6]. However this optimization process is done for one part medium. Devaney and a group of researcher worked on an inverse problem for two part medium as he did in [3] but the important difference was the algorithm for reconstruction which was likelihood [6].

In geophysical imaging; another suggestive work was made by Alan Witten and John E. Molyneux [8]. It declares an algorithm for a configuration in which a finite number of sources and receivers of arbitrary character are allocated along one line having an arbitrary orientation with respect to the each other as an application of diffraction

tomography. If the number of the sources increases; it improves the results observably. But this work does not take layered medium into account. [9] which is prepared by Chaturvedi and Plumb, is also a basic research for this thesis. The source & observer configuration and the location of the object are almost same with the problem used in the content of this thesis. However in [9] forward problem is evaluated by FDTD; and after that an iterative method based on Born approximation, Born iterative, is used for solving the inverse problem.

Lastly there are more suggestive published studies about this subject. [10, 11] develop a regularized recursive linearization method for 2-D near field inverse scattering problem. [10] is based on multiple frequency scattering data. They take the Born approximation as a starting point in inverse problem which corresponds to weak scattering at low frequencies. Then they update the solution with a recursive linerization. Besides, they explained the mathematical models of numerical methods and solution of Green's function clearly which make the study a simple guide [10].

Another work which consists of a solution on inverse-scattering problem within the second-order Born approximation by means of a two-step inexact-Newton algorithm is made by an Italian group. The reconstruction process, the approximations are supported by good numerical examples which can be indicative for this thesis [12].

1.3 The Purposes and the Organization of the Thesis

Although the above mentioned studies have made valuable contributions to the problems that are concerned with this thesis, some additional analysis and alternative approaches can be made connected to these problems. So that, the main objective of this thesis is a comparatively analysis of a well known inverse problem explained in section 1.1 and 1.2, related to the dielectric objects buried in a two half space medium by two different methods (Born and Newton Method) and the investigation of the effects of some electromagnetic parameters subject to the mentioned inverse scattering problem. Another purpose of this framework is to determine the contributions of the different source and receiver configurations by the same methods, i.e; Born and Newton Methods.

Furthermore, in order to state the limits of the methods as well as to see the effects of some parameters such as number of sources, frequency, size of reconstruction domain, depths of the buried objects etc. on the solution for the actual problem is the most important aim. The organization of the thesis is as follows below.

Firstly, section 2 will start by the definition of the scattering problem. Then the Green's function will be determined for near-field scattering problem in a lossy and inhomogeneous medium which is planarly interfaced to two parts as free space and underground. After Green's function is stated; a numerical method called MoM (method of moments) will be used in order to calculate the scattered field data according to the physical properties and the geometry of the scattering object. This process will give the scattering data or the measurement data where the forward problem ends.

Secondly; some approches will be introduced while starting to the inverse problem, section 3. Then the measurement data (scattered field data) which is found in forward problem, will be used in the reconstruction process to find out the location, the shape and the characteristic parameters of the dielectric object buried underground. In this reconstruction procedure; two methods will be applied: Born and Newton Method. Furthermore we will try to improve these methods by using the advantages of the problem's configuration.

In section 4; according to the methods and approaches different kind of numerical applications are done to analyse the methods subject to purposes mentioned.

The conclusion of this thesis is presented in section 5 with some discussions.

2. FORWARD PROBLEM

Forward problem consists of the solution of Green's function and then evaluation of numerical method MoM to create measurement data from the known geometry of the dielectric buried object. But before starting to the solution of the Green's fuction; let's look at the definition and formulation of the scattering problem.

2.1 The Definition of the Scattering Problem

If there is any wave propagation in the presence of the scatterers (objects, obstacles) of different geometries, it can be referred as scattering. So that, the total field ($\overrightarrow{E_t}$, $\overrightarrow{H_t}$) become the superposition of the scattering fields ($\overrightarrow{E_s}$, $\overrightarrow{H_s}$) with the incident (direct) fields ($\overrightarrow{E_i}$, $\overrightarrow{H_i}$) [13].

$$\overrightarrow{E_t} = \overrightarrow{E_i} + \overrightarrow{E_s} \quad \textbf{(2.1)}$$

$$\overrightarrow{H_t} = \overrightarrow{H_i} + \overrightarrow{H_s} \quad \textbf{(2.2)}$$

It is known that the incident fields ($\overrightarrow{E_i}$, $\overrightarrow{H_i}$) is the function of the source, in other words it is the Green's function. So if the expression of scattered field is explained, we can acquire the total field. If we take the electric field parameter; we can write the wave equations according to a current source radiating in the vicinity of a general inhomogenity. Using the geometry and parameters in Figure 1.1; the total field can be written as;

$$\overrightarrow{E_t}(x) = \overrightarrow{E_i}(x) + \int_D G(x;y)\left(k_{obj}^2 - k_2^2\right)\overrightarrow{E_t}(y)dy \quad \textbf{(2.3)}$$

where, k_{obj} and k_2 are the wave numbers for object and 2nd medium

$$k_{obj} = w\sqrt{\varepsilon_{obj}\ \mu_{obj} + \frac{i\sigma_{obj}\ \mu_{obj}}{w}} \quad \textbf{(2.4)}$$

$$k_2 = w\sqrt{\varepsilon_2\ \mu_2 + \frac{i\sigma_2\ \mu_2}{w}} \quad \textbf{(2.5)}$$

$\overrightarrow{E_i}(x)$: Incident field in x measurement points,

$\overrightarrow{E_t}(y)$: Total field in D region

$G(x;y)$: Green function in x measurement points for y points in D region

So from the integral equation above; it can be said that (it has the same procedure for $\vec{H}$ field)

$$\overrightarrow{E_s}(x) = \int_D G(x;y)\left(k_{obj}^2 - k_2^2\right)E_t(y)dy \quad \textbf{(2.6)}$$

where $\overrightarrow{E_s}\ (x)$ is the scattered field in x measurement points.

To find the scattered fields step by step; we can start from the solution of the Green's function for the geometry of Figure 1.1 [14].

2.2 Green's Function of the Two-Part Space with Planar Interface

Green's function can be explained as the source function of our configuration. We will solve the Green's function by Fourier transform method.

Let our Green's function be $G(x;y)$ in rectangular cordinate system. By the definition of the Green's function equation, $G(x;y)$ should satisfy ;

$$\Delta G(x;y) + k^2(x_2)\ G(x;y) = -\delta(x-y) \quad \textbf{(2.7)}$$

under the radiation condition. k is a function of x_2 , $x, y \in \mathbb{R}^2$, and δ is Dirac's delta distribution. The fourier transform of Green's function with respect to x_1 is;

$$\hat{G}(\nu, x_2;\ y) = \int_{-\infty}^{+\infty} G(x;y)e^{-i\nu x_1}dx_1 \qquad \textbf{(2.8)}$$

So if we take the fourier transform of the both sides of equation 2.7 ;

$$\frac{\partial^2 \hat{G}}{\partial x_2^2} + \int_{-\infty}^{+\infty} \frac{\partial^2 G}{\partial x_1^2} e^{-i\nu x_1}dx_1 + k_j^2 \hat{G} = \int_{-\infty}^{+\infty} -\delta(x_1 - y_1)\delta(x_2 - y_2)e^{-i\nu x_1}dx_1 \qquad \textbf{(2.9)}$$

$$\frac{d^2 \hat{G}}{dx_2^2} - (\nu^2 - k_j^2)\hat{G} = -\delta(x_2 - y_2)e^{-i\nu y_1} \qquad \textbf{(2.10)}$$

where,

j = 1, 2 ; $\nu \in C_R$; $\hat{G}$ and $\frac{\partial \hat{G}}{\partial x_2}$ are continuous on $x_2 = 0$ [15].

C_R is the regularity line for $\hat{G}$ in the complex ν plane. According to configuration in Figure 1.1 ; our source which has the cordinates $(y = y_1, y_2)$ is in the region $x_2 < 0$; make the differential equation 2.10 as below.

$$\frac{d^2 \hat{G}}{dx_2^2} - \gamma_1^2 \hat{G} = 0 \qquad \textbf{(2.11)}$$

$$\frac{d^2 \hat{\mathrm{G}}}{dx_2^2} - \gamma_2^2 \hat{\mathrm{G}} = -\delta(\, x_2 - y_2\,)e^{-i\nu y_1} \qquad \textbf{(2.12)}$$

where, $\gamma_j = \sqrt{\nu^2 - k_j^2}$; j = 1, 2 **(2.13)**

The general solution will be $e^{\pm \gamma x}$; additionally in order to solve the differential equations, we will use A, B, C and D coefficients.

$$\hat{G}(\nu, x_2 ; y_1, y_2) = \begin{cases} A(v)e^{-\gamma_1 x_2} & ; \quad x_2 > 0 \\ B(v)e^{-\gamma_2 x_2} + C(v)e^{\gamma_2 x_2} & ; \quad y_2 < x_2 < 0 \\ D(v)e^{\gamma_2 x_2} & ; \quad x_2 < y_2 \end{cases} \quad \textbf{(2.14)}$$

We have 4 unknowns; so that we will need 4 equations to solve it. We should write these equations according to the boundary conditions.

$\hat{G}(\nu, x_2 = 0^+ ; y) - \hat{G}(\nu, x_2 = 0^- ; y) = 0$ [Ē cont.] **(2.15)**

$\frac{\partial \hat{G}}{\partial x 2}(v, x_2 = 0^+; y) - \frac{\partial \hat{G}}{\partial x 2}(v, x_2 = 0^-; y) = 0$ $[\overrightarrow{H}\ cont., \mu_1 = \mu_2]$ **(2.16)**

$\hat{G}(\nu, x_2 = y_2 + 0 ; y) - \hat{G}(\nu, x_2 = y_2 - 0 ; y) = 0$ [Ē cont.] **(2.17)**

$\frac{\partial \hat{G}}{\partial x 2}(v, x_2 = y_2 + 0; y) - \frac{\partial \hat{G}}{\partial x 2}(v, x_2 = y_2 - 0; y) = e^{-ivy_1}$ $[\overrightarrow{H}\ cont., \mu_1 = \mu_2]$ **(2.18)**

After using the boundary conditions; we can find A, B, C, D.

$$A(v) = \frac{2\gamma_2}{\gamma_1 + \gamma_2} \frac{1}{2\gamma_2} e^{-ivy_1} e^{\gamma_2 y_2} \quad \textbf{(2.19)}$$

$$B(v) = \frac{1}{2\gamma_2} e^{-ivy_1} e^{\gamma_2 y_2} \quad \textbf{(2.20)}$$

$$C(v) = \frac{\gamma_2 - \gamma_1}{\gamma_1 + \gamma_2} \frac{1}{2\gamma_2} e^{-ivy_1} e^{\gamma_2 y_2} \quad \textbf{(2.21)}$$

$$D(v) = \frac{1}{2\gamma_2} e^{-ivy_1} e^{-\gamma_2 y_2} + \frac{\gamma_2 - \gamma_1}{\gamma_1 + \gamma_2} \frac{1}{2\gamma_2} e^{-ivy_1} e^{\gamma_2 y_2} \quad \textbf{(2.22)}$$

The next step should be the determination of Green's function by taking the inverse Fourier transform of $\hat{G}$ with respect to equation (2.23) .

$$G(x; y) = \frac{1}{2\pi}\int_{C_R} \hat{G}(v, x_2; y)e^{iv\,x_1}\,dv \qquad \textbf{(2.23)}$$

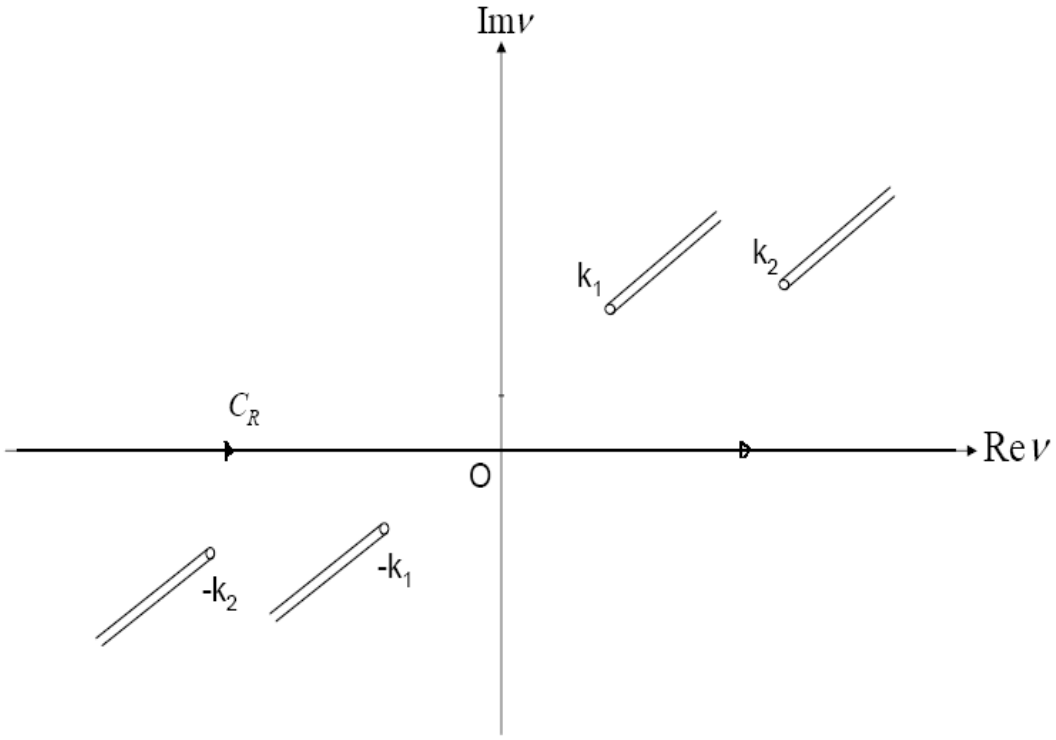

Figure 2.1 : Regularity line of $\hat{G}$ in the complex v Plane.

In this thesis, we will always work on lossy space configurations. It is same even for free space. The conductivity of free space will be taken 10^{-10}. Consequently; the conductivities for the two parts of space $\sigma_{1,2} \neq 0$. That means, while taking the complex integral, the regularity line C_R will be as in Figure 2.1 [16]. (C_R is on $Re\vartheta$ axis.) Besides, according to the geometry in Figure 1.1 ($x_2 < 0, y_2 < 0$); we will use B, C and D coefficients. Thus Green's function can be expressed as;

$$G(x;y) = G_1(x;y) + G_2(x;y) \quad \textbf{(2.24)}$$

where,

$$G_1(x;y) = \frac{1}{2\pi}\int_{C_R} \frac{1}{2\gamma_2} e^{iv(x_1-y_1)} e^{-\gamma_2|x_2-y_2|}\, dv \quad \textbf{(2.25)}$$

$$G_2(x;y) = \frac{1}{2\pi}\int_{C_R} \frac{\gamma_2-\gamma_1}{\gamma_1+\gamma_2}\frac{1}{2\gamma_2} e^{iv(x_1-y_1)} e^{\gamma_2(x_2+y_2)}\, dv \quad \textbf{(2.26)}$$

$G_1(x;y)$ is the is the directly transmitted wave and it can be expressed in terms of zero order Hankel function of the first kind $H_0^{(1)}$ which can be found by the solution of the scalar wave equations in cylindirical cordinate system [13]. Therefore equation (2.27) can be a test model for the integral expression of $G_1(x;y)$. Because a numerical integration method will be used for the integrals above; where the algorithm and the boundaries of the integrals must be determined. It will also help us to see the accuracy and validation limits of numerical integration. So if we compare the integral equations with the analytic results for the icident fields; we should determine the parameters of the integral equations. There is a MATLAB simulation result for the comparison subject to equation (2.27), below.

$$\frac{i}{4}H_0^{(1)}(k_2|x-y|) = \frac{1}{2\pi}\int_{C_R} \frac{1}{2\gamma_2} e^{iv(x_1-y_1)} e^{-\gamma_2|x_2-y_2|}\, dv \quad \textbf{(2.27)}$$

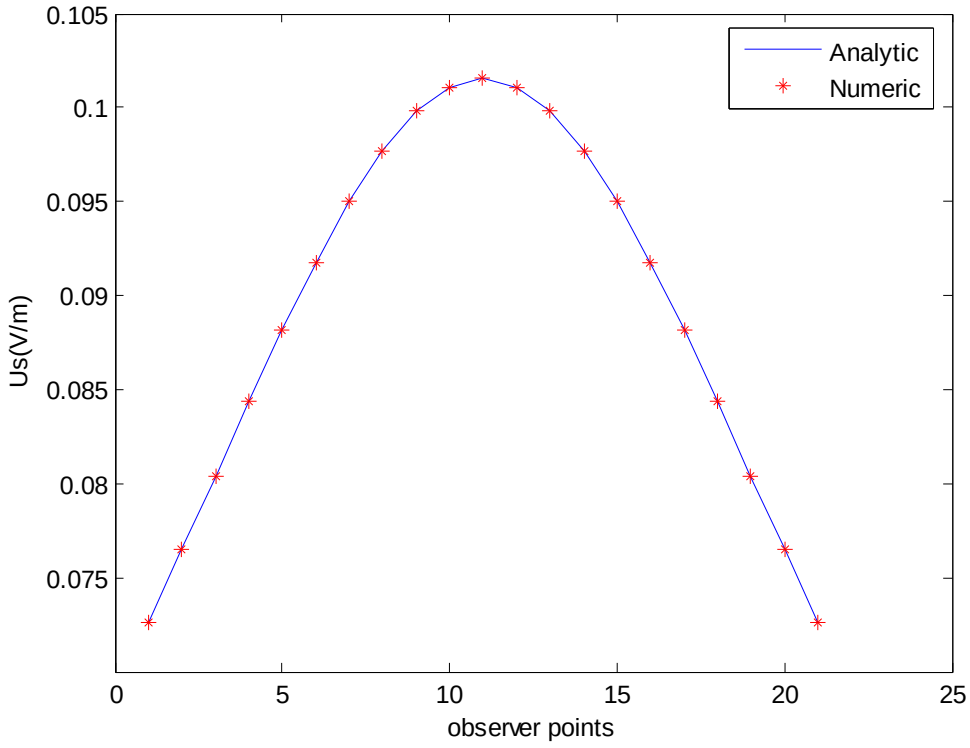

Figure 2.2 : Comparison between analytical $H_0^{(1)}$ and numerical G_1

MATLAB *'quad'* function which is based on adaptive Simpson quadrature is used for the numerical integration. It has an 10^{-6} error tolerance. The bounds for the numerical integration is choosed as $\pm 20Re(k_1)$. The source and the observers are symetrically located according to configuration in Figure 1.1 by ignoring the object. k_1 is free space, k_2 is considered as dry soil. (relative dielectric constant and conductivity of soil is $\varepsilon_2 = 3,\ \sigma_2 = 10^{-3}$ respectively) From the Figure 2.2 it can be seen that; the numerical integration gives almost the exact solution of analytical $H_0^{(1)}$ for the given parameters. So for the simulations next; this comparison will be taken into consideration in the evaluation of $G_2(x;y)$ besides instead of $G_1(x;y)$ we will use $H_0^{(1)}$. So our Green's function will be;

$$G(x;y) = \frac{i}{4}H_0^{(1)}(k_2|x-y|) + \frac{1}{2\pi}\int_{C_R}\frac{\gamma_2-\gamma_1}{\gamma_1+\gamma_2}\frac{1}{2\gamma_2}e^{iv(x_1-y_1)}e^{\gamma_2(x_2+y_2)}\,dv. \qquad \textbf{(2.28)}$$

2.3 MoM Solution for the Scattered Field

Let u_i be the incident field, u_s be the scattered field and u be the total field. If we rewrite the equation (2.3), it will be ;

$$u(x) = u_i(x) + k_2^2 \int_D G(x;y)\, v(y) u(y) dy \qquad \textbf{(2.29)}$$

where $v(y)$ stands for the object function for region D.

$$v(y) = \frac{k_{obj}^2(y)}{k_2^2(y)} - 1 \qquad \textbf{(2.30)}$$

The part with the integral form of the equation 2.29 is the expression of the scattered field which is a second kind Fredholm integral equation. The left side of the equation is the total field $u(x)$ at the x measurement points, however there is u(total field) for D region again in the right side of the equation. Therefore the equation 2.29 is non-linear. In order to solve this equation directly for the forward problem, we should use a numerical method to handle the non-linearity.

If we get back to problem; in order to apply the numerical method to our D region (our object) we will divide our object into M x N cells. After the divison we can use superposition for all cells under some useful approximations [17].

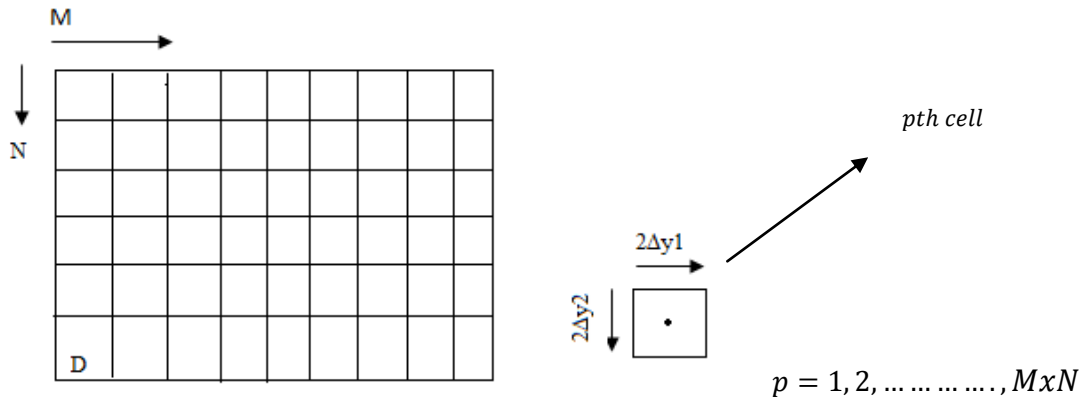

Figure 2.3 : Division of D region

If we write the total field equation in terms of the cell parameters;

$$u(x) = u_i(x) + k_2^2 \sum_{p=1}^{MxN} \int_{D_p} G(x; y^p)\, v(y^p) u(y^p) dy \quad \textbf{(2.31)}$$

While we are taking the each cell's integral; we will take the center points of cell's as reference. Therefore the total field $u(y^p)$ for pth cell will be taken according to the center point y^p. We will need an important approximation here for the total field. We should choose each cell (D_p's) small enough that all the points in D_p cell will be equal to the other points in the same cell; $u(y) \cong u(y^p)$ where the center point $y^p = y_1^p, y_2^p$ for the cell D_p . Moreover the object function will be taken same for all cells; $v(y^p) = v$.

$$u(x) = u_i(x) + k_2^2 \sum_{p=1}^{MxN} v(y^p) u(y^p) \int_{D_p} G(x; y^p)\, dy \quad \textbf{(2.32)}$$

In order to catch an expression of total field; we should use the $y^{p'}$ points for D_p cells in D region instead of x measurement points, which could handle non-linearity after some operations.

$$u\left(y^{p'}\right) = u_i\left(y^{p'}\right) + k_2^2 \sum_{p=1}^{MxN} v(y^p) u(y^p) \int_{D_p} G\left(y^{p'}; y^p\right) dy\,; \;\; p' = 1, 2, \ldots\ldots, MxN \quad \textbf{(2.33)}$$

After some algebraic operations, we can write the equation (2.33) in matrix form;

$$[I - A] u\left(y^{p'}\right) = u_i(y^{p'}) \quad \textbf{(2.34)}$$

where I is the identity matris and

$$A_{p'p} = k_2^2 v \int_{D_p} G\left(y^{p'}; y^p\right) dy. \quad \textbf{(2.35)}$$

$$C^p(y^{p'}) = \int_{D_p} G\left(y^{p'}; y^p\right) dy \quad \textbf{(2.36)}$$

The Green's function, found in section 2.2, will be used in equation (2.35) and (2.36). We can write the integral form in equation (2.35) as coefficients for the rectangular cells with the side lengths $2\Delta y_1$ x $2\Delta y_2$ in eq. (2.36).

$$C_1^p\left(y^{p'}\right) = \int_{D_p} G_1\left(y^{p'}; y^p\right) dy \; ; \tag{2.37}$$

$$C_2^p\left(y^{p'}\right) = \int_{D_p} G_2\left(y^{p'}; y^p\right) dy \tag{2.38}$$

$$C_1^p\left(y^{p'}\right) = \begin{cases} \frac{i}{2k_2^2}\left[\pi k_2 a H_1^1(k_2 a) + 2i\right], & p = p' \\ \frac{i\pi a}{2k_2} J_1(k_2 a) H_0^1\left(k_2 \left| y^{p'} - y^p \right|\right), & p \neq p' \quad [5] \end{cases} \tag{2.39}$$

$$C_2^p\left(y^{p'}\right) = \frac{2}{\pi}\int_{C_R} \frac{\gamma_2 - \gamma_1}{\gamma_1 + \gamma_2} \frac{1}{2\gamma_2} \frac{\sinh(\gamma_2 \Delta y_2)}{\gamma_2} \frac{\sin(v\Delta y_1)}{v} e^{iv\left(y_1^{p'} - y_1^p\right)} e^{\gamma_2\left(y_2^{p'} + y_2^p\right)} dv \tag{2.40}$$

'a' is the radius of a circular cell whose area is equal to the any rectangular cell D_p of D region . By using the coefficients C_1 , C_2 ; $[I - A]$ can be found. A is a PxP' square matrix. Then the equation 2.34 will be;

$$u\left(y^{p'}\right) = [I - A]^{-1} u_i\left(y^{p'}\right) \tag{2.41}$$

The inverse matrix is known, the incident fields which are our Green's function at points $y^{p'}$ is known; so we can find the total field $u\left(y^{p'}\right)$ inside the D region. After finding the fields inside D region, we can find scattered field at any point; just by replacing the measurement points from $y^{p'}$ to the any x point. This is where the forward problem process ends.

$$u_s(x) = k_2^2 \sum_{p=1}^{MxN} v(y^p) u(y^p) \left(C_1^p(x) + C_2^p(x)\right) \tag{2.42}$$

2.4 Comparison of Numerical and Analytical Method

After finding scattered field; the numerical method should be checked in order to choose reasonable values for the parameters; like the object size, frequency, cell size etc. We will check the numerical method on a dielectric cylinder which we know the analytic solution of it. The analytical solution won't be detailed here but it can be found in [13,16]. So for a good comparison, by using a radius function we should create a cross section of a cylinder from the rectangular cells.

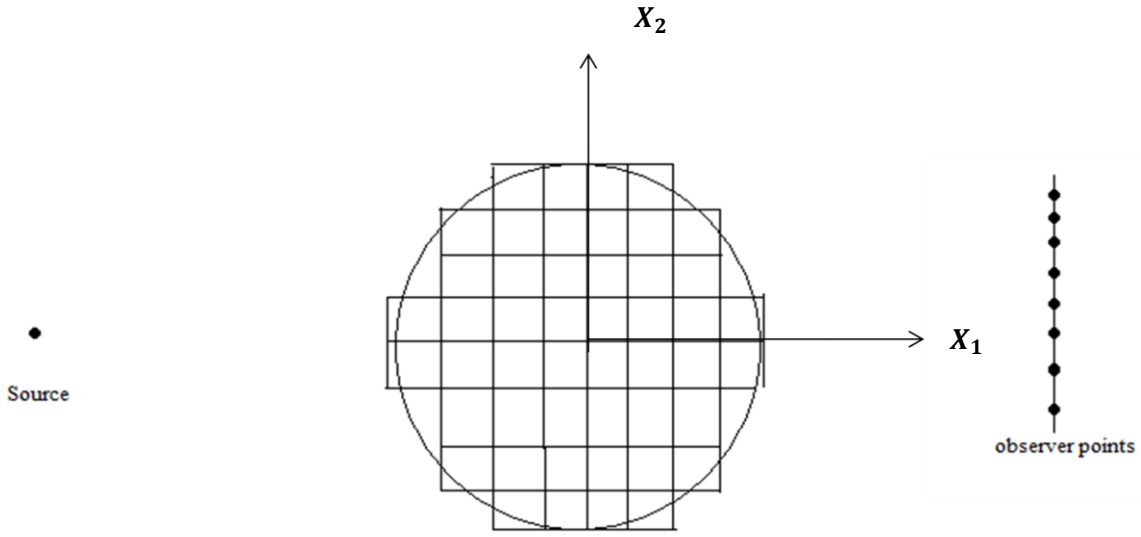

Figure 2.4: The configuration for the comparison

As it can be seen from the configuration, the test will be done for one part medium. Then our $G_2(x;y)$, $C_2^p(x)$ will be ignored.

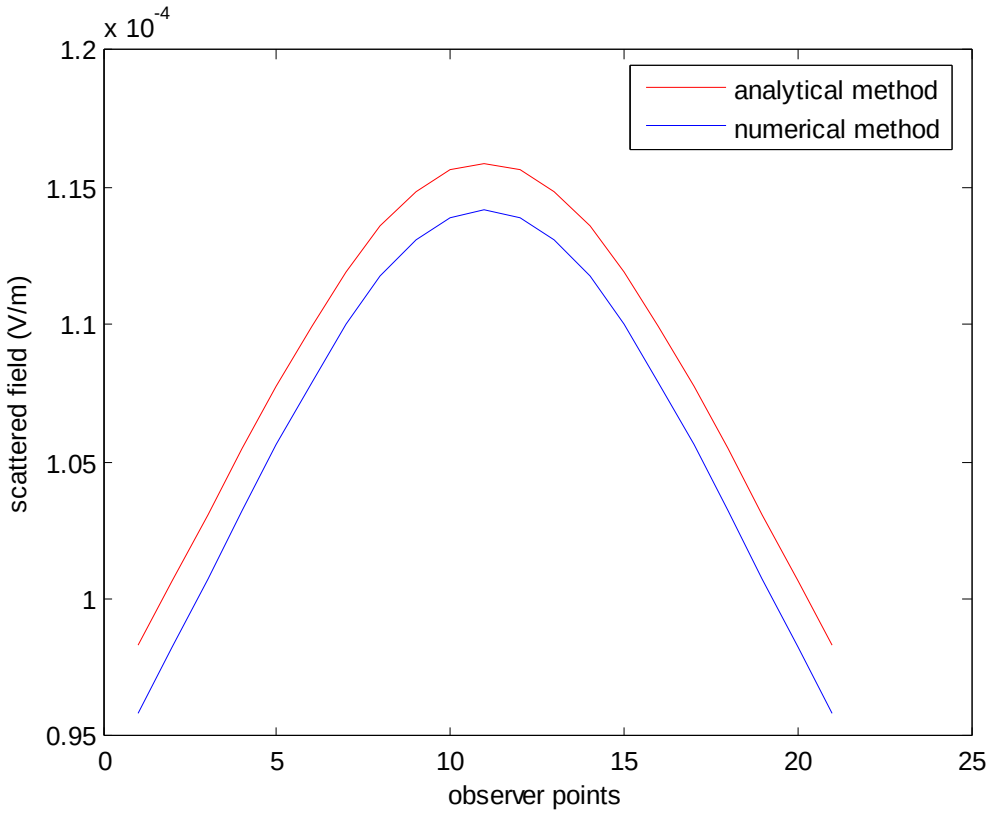

Figure 2.5: Comparison of analytical and numerical method for a dielectric cylinder

A diectric cylinder whose radius is $r = 1m$ and has relative dielectric constant and conductivitiy $\varepsilon_{obj} = 4$, $\sigma_{obj} = 10^{-7}$ $(\frac{S}{m})$ respectively. The parameters of the medium are $\varepsilon = 3$, $\sigma = 10^{-5}$ $(\frac{S}{m})$. Magnetic permeability of the medium and the dielectric cylinder are same with free space. Generally all the simulations for this thesis will be done for a frequency interval $10\,MHz \leq f \leq 50\,MHz$; which brings important advantages according to higher frequencies. For the present simulation $f = 10\,MHz$. The cell sides are chosen $\frac{\lambda_{obj}}{20} x \frac{\lambda_{obj}}{20}$. These values for cell sides are our upper limits; if we choose greater than these values, the results are worse. However if we choose smaller than this, it brings almost same results with more computational cost. Unless otherwise is stated, they will be choosen same for the simulations next. The source and the observer lines are symmetric with respect to the dielectric cylinder. The cordinates of

source (-5, 0) and the observer points which start from (5,5), until (5,-5) with 21 points equally. From Figure 2.5 it can be seen that the results(absolute value of scattered field with respect to observer points) are very close to each other. The numerical method has an error about 3% compared to analytical method. This error may come from the modeling of the circular cylinder with rectangular cells besides 3% error can be allowable for the simulations next.

This test is suggestive for us about the solution of the forward problem. Now we can start to inverse problem which this thesis is interested more ,by using the measurement data acquired from the forward problem. Whereas in the practical application you don't have to solve a forward problem; since you measure the scattered field and use the real measurement data in the reconstruction process.

3. INVERSE PROBLEM

Inverse scattering problem is the problem of determining the characteristics of an object (its shape, internal constitution, etc.) from measurement datas of radiation or particles scattered from the object. To make it clear; the place of the sources and observers are known while the object location is not. In order to find the location, shape and characteristics of the object; one should investigate a region bigger than object to find the object in that region. It is called reconstruction or investigation domain. The measurement datas found from section 2 will be used for the evaluation of inverse problem so that the results can be compared with a true profile of the object. There are different algorithms such as Born, Rytov, distorted Born, Born iterative, Newton iterative algorithms for inverse problems. Born and Newton Method will be explained basically; moreover an optimization process by using multiple sources for both methods will be told. Born Method is a really basic method for inverse problems where we will start from.

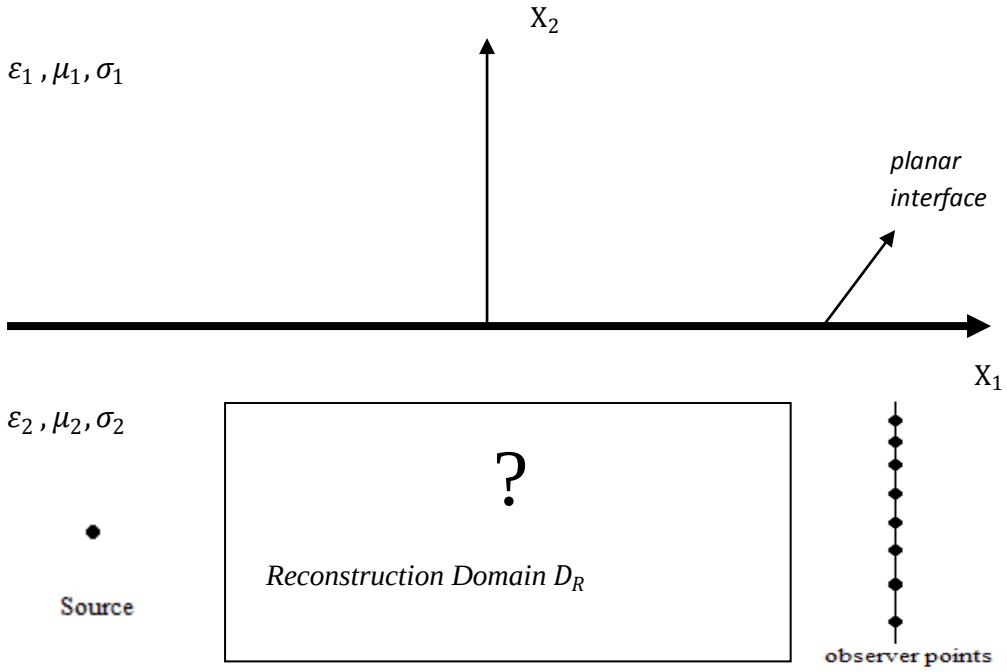

Figure 3.1: Geometrical configuration for reconstruction domain

3.1 Born Approximation

In scattering theory, the Born approximation consists of taking the incident field in place of the total field as the driving field at each point in the scatterer. It is the perturbation method applied to scattering by an extended body [19]. This method works for 'weak scattering problems'. Because while finding the scattering field by the integral equation (2.29); the total field is used. So if the scattered field is very small compared to the total field; one can ignore the scattering field and use the incident field instead of total field in the integral equation.

3.1.1 Formulation of the Born Method

The Born approximation is a "weak scattering approximation" and requires that the total scattered field be small in comparison with the incident field. This, in turn, requires that both the magnitude of the object profile and the total extent of object volume be small

[7]. Therefore for the formulation, we will change the equation (2.29) by changing the total field u by u_i and D by D_R .

$$u_s(x) = k_2^2 \int_{D_R} G(x;y)\, v(y) u_i(y) dy \qquad \textbf{(3.1)}$$

From the formula above; $u_s(x)$ which is the scattered field data at x points is known. y points are the points in the domain of reconstruction D_R . $G(x;y)$ is the Green's function for the reconstruction domain. $u_i(y)$ is the incident field at the reconstruction domain; which radiates from a fixed source point. So the only unknown is $v(y)$ which is the object function in D_R domain. If the coefficient equations whose solution is given in section 2, are applied to the reconstruction domain and multiplied by u_i ; a matrix which has the information about the object function will be acquired [18].

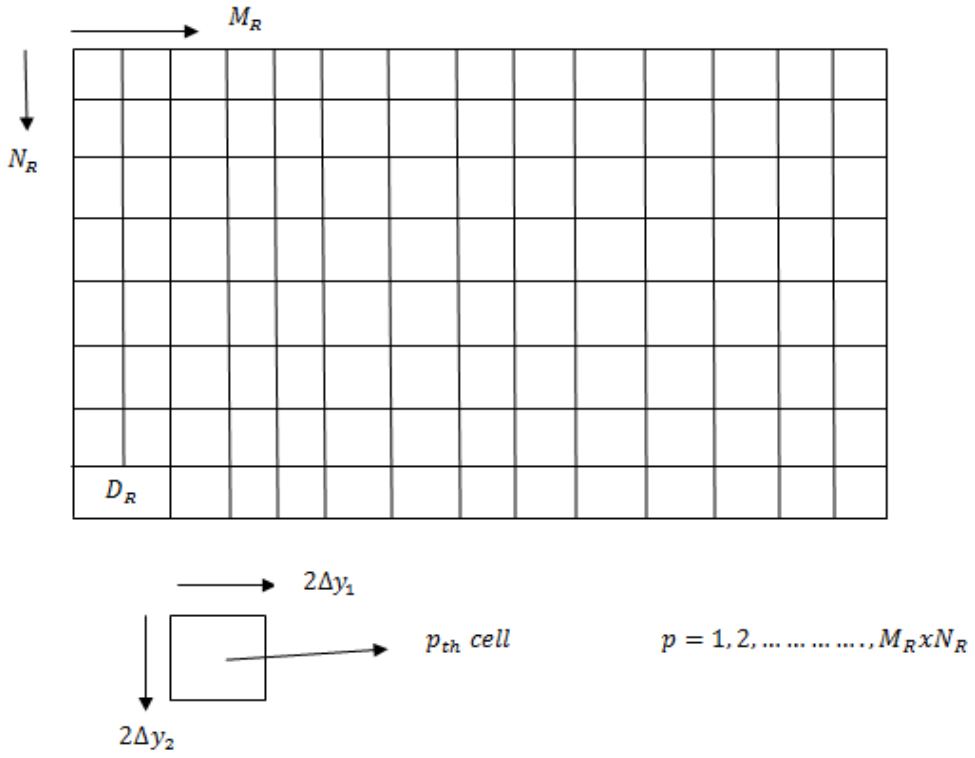

Figure 3.2 : Division of recontruction domain into cells for numerical solution

$$u_s(x) = k_2^2 \sum_{p=1}^{M_R x N_R} v(y^p) u_i(y^p) \int_{D_{R_p}} G(x; y^p)\, dy \quad \textbf{(3.2)}$$

$$C_1^p(x) = \int_{D_{R_p}} G_1(x; y^p) dy \; ; \qquad C_2^p(x) = \int_{D_{R_p}} G_2(x; y^p) dy \quad \textbf{(3.3)}$$

$$C^p(x) = C_1^p(x) + C_2^p(x) \quad \textbf{(3.4)}$$

From equation (3.2) to (3.4), can be derived from section 2, MoM solution depending on the structure in Figure 3.2. The basic difference is that, we apply the Born Method to the reconstruction domain. x is the measurement point; so if x is changed by a Γ observation line which consists of R points to increase the data; we will have an A matrix as showed below.

$$A_{rp} = k_2^2\, u_i(y^p) \int_{D_{R_p}} G(x^r; y^p) dy \;\; ; \; r = 1, 2, \dots, R \quad \textbf{(3.5)}$$

If we use equation (3.5) in the scattered field formula in equation (3.2); a matrix solution of v object profile can be found easily.

$$Av = u_s \quad \Rightarrow \quad v = A^{-1} u_s \quad \textbf{(3.6)}$$

However the inverse of the matrix A which is R x P for the present problem, does not exist. This is a typical problem of inverse problems called ill-posed problems. Thus; A needs to be a regularized. Tikhonov Regularization is applied to handle this ill-passed problem [19]. Also it will be applied for all ill-possed problems in this thesis.

$$\alpha I + A^* A v = A^* u_s \quad \textbf{(3.7)}$$

Firstly; the conjugate transpose of matrix A is multiplied by both sides of the first part of equation (3.6). But it is not enough for a good regularization; so that αI is added to it where I is the identity matrix and α is a scaling parameter and $0 \leq \alpha < 1$. $\alpha = 0$ is an ideal condition however for the practical applications it is better if it is chosen very

small. The small values chosen for α can be an indication to the ill-posed character of the problem. Consequently the object profile will be;

$$v = (\alpha I + A^* A)^{-1} A^* u_s \quad \textbf{(3.8)}$$

3.1.2 Multi-source Effect on Born Method

The analysis of the multi-source effect is an important part of this thesis. Since the data number for the fixed equations will increase by the multi-source effect, it effect should bring better solutions. The formulation of the multi-source should be;

$$u_s(x^r, z^q) = k_2^2 \sum_{p=1}^{M_R x N_R} v(y^p) u_i(y^p, z^q) \int_{D_{R_p}} G(x^r; y^p)\, dy \quad \textbf{(3.9)}$$

where observation points $x^r and\, r = 1,2, \ldots\ldots, R$ and source points z^q and $q = 1,2, \ldots\ldots, Q$ and y^p's are center points of the cell D_p's in D region where $p = 1,2, \ldots\ldots, P$.

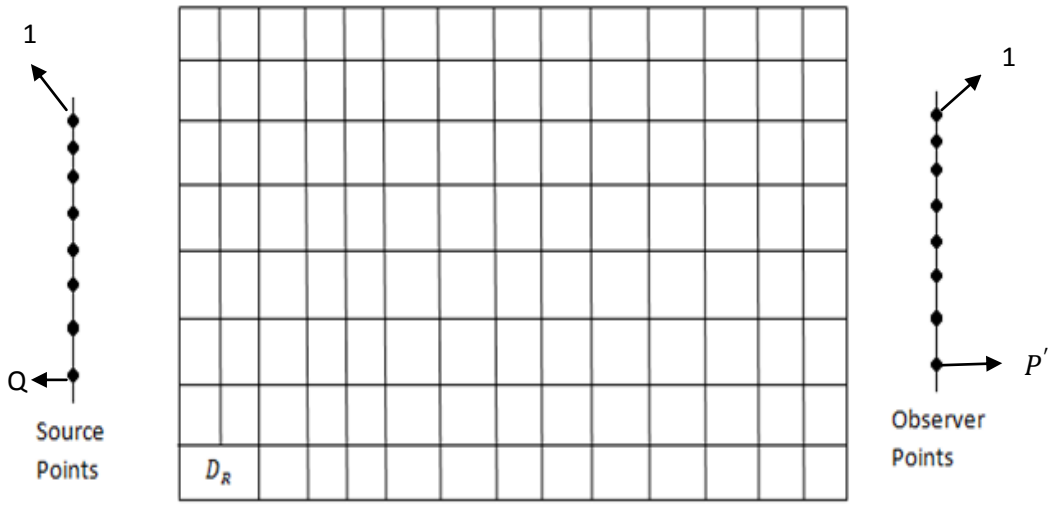

Figure 3.3: Multiple source configuration for the same reconstruction domain

So the A matrix in the formulation part will be for the multi-source Born as;

$$A_{tp} = k_2^2\, u_i(y^p, z^q) \int_{D_{R_p}} G(x^r; y^p) dy \quad \textbf{(3.10)}$$

where $t = (r, q)$

If we write it in the matrix form;

$$A = \begin{bmatrix} k_2^2\, u_i(y^1,z^1)\int_{D_1} G(x^1;y^1)dy & k_2^2\, u_i(y^2,z^1)\int_{D_2} G(x^1;y^2)dy & \dots & k_2^2\, u_i(y^p,z^1)\int_{D_p} G(x^1;y^p)dy \\ k_2^2\, u_i(y^1,z^1)\int_{D_1} G(x^2;y^1)dy & k_2^2\, u_i(y^2,z^1)\int_{D_2} G(x^2;y^2)dy & \dots & k_2^2\, u_i(y^p,z^1)\int_{D_p} G(x^2;y^p)dy \\ \dots\dots & \dots\dots & & \dots\dots \quad \dots\dots \\ \dots\dots & \dots\dots & & \dots\dots \quad \dots\dots \\ k_2^2\, u_i(y^1,z^1)\int_{D_1} G(x^r;y^1)dy & k_2^2\, u_i(y^2,z^1)\int_{D_2} G(x^r;y^2)dy & \dots & k_2^2\, u_i(y^p,z^1)\int_{D_p} G(x^r;y^p)dy \\ k_2^2\, u_i(y^1,z^2)\int_{D_1} G(x^1;y^1)dy & k_2^2\, u_i(y^2,z^2)\int_{D_2} G(x^1;y^2)dy & \dots & k_2^2\, u_i(y^p,z^2)\int_{D_p} G(x^1;y^p)dy \\ \dots\dots & \dots\dots & & \dots\dots \quad \dots\dots \\ k_2^2\, u_i(y^1,z^Q)\int_{D_1} G(x^{P'};y^1)dy & k_2^2\, u_i(y^2,z^Q)\int_{D_2} G(x^{P'};y^2)dy & & \dots\dots \quad \dots\dots \end{bmatrix}$$

$$Av = u_s \qquad \textbf{(3.11)}$$

The matrix A goes until rth row for the first source. After rth row the same process start for the second source $q = 2$. The last row is $2r$ for the second source, it continues for the last source. So the matrix size depends on the source and the observer numbers as it depends on the cell numbers of the reconstruction domain. A is $(R \text{ x } Q)$ x (P), v is (P x 1) and u_s is $(R \text{ x } Q)$ x 1. Multi-source Born approximation is still ill-posed problem so that it needs regularization which Tikhonov regularization is used.

$$v = (\alpha I + A^* A)^{-1} u_s \qquad \textbf{(3.12)}$$

3.2 Newton Method

Newton Method is an iterative approach by starting from an initial guess of the unknown object function which is used for the solution of the inverse scattering problems. This method is more complex compared to the Born method. In Born Method, since the scattered field is ignored in the second kind Fredholm integral equation; some informations are missed. That effects result's of for Born negative; however in Newton

Method; by the help of the initial guess and the measurement data; in each iteration; the inverse solution got close to the object function [20].

3.2.1 Formulation of the Newton Method

Let $F(v)$ which is a non-linear functional, be an operator. $F(v) = u_s$ can be an expresion from the second kind Fredholm integral equation.

$$F(v) = k_2^2 \int_D G(x;y)\, v(y) u(y) dy \qquad \textbf{(3.13)}$$

where observation points $x \in \Gamma$ observation line.

Equation (3.13) is a non-linear equation for the object function v. As mentioned this equation can be solved through a linearization in the Newton's procedure. By using the Fréchet derivative and an initial guess $v^{(0)}$; one can linearize the equation above.

$$F\left(v^{(0)}\right) + F'\left(v^{(0)}\right)\delta v^{(1)} = u_s \qquad \textbf{(3.14)}$$

where $F\left(v^{(0)}\right) = k_2^2 \int_D G(x;y)\, v^{(0)}(y) u^{(0)}(y) dy$ can be written from equation (3.13) . $v^{(0)}$ is the initial guess thus for the solution of $F\left(v^{(0)}\right)$, $u^{(0)}$ is needed to be found. It will be found as it is done in section 2; the main difference will be the change of the domains. Now $u^{(0)}$ will be solved for reconstruction domain;

$u^{(0)}\left(y^{p'}\right) = [I - A]^{-1} u_i(y^{p'})$ where p' are the center point of any $D_{p'}$ cell, in other words measurement points for D_R and equation (2.35) becomes $A_{p'p} = k_2^2 v^{(0)} \int_{D_{R_p}} G\left(y^{p'}; y^p\right) dy$. After finding the fields $u\left(y^{p'}\right)$ inside the D_R region, $F\left(v^{(0)}\right)$ is found from the equation (3.13). The solutions of the integrals are shown in section 2.3 .

For the Fréchet derivative, from the definition of it;

$$F'\left(v^{(0)}\right)\delta v^{(1)} \triangleq k_2^2 \int_D G(x;y)\, u^{(0)}(y) \delta v^{(1)} dy \qquad \textbf{(3.15)}$$

so if equation (3.15) is used in the linearization, then the equation will be;

$$k_2^2 \int_D G(x;y)\, u^{(0)}(y)\delta v^{(1)} dy = u_s(x) - F\left(v^{(0)}\right) \quad \textbf{(3.16)}$$

$u_s(x)$ is the measurement data while $F\left(v^{(0)}\right)$ is the determined one from equation (3.13).

$$B_{rp} = k_2^2 \int_{D_{R_p}} G(x^r; y^p) u^{(0)}(y^p) dy \quad \textbf{(3.17)}$$

where x^r is an observation point and $r = 1,2, \ldots R$ and p is the cell number of D_R as it is used to be in section 3. B is $R \times P$ matrix where the size of $\delta v^{(1)}$ is $P \times 1$. $\delta v^{(1)}$ can be solved by the matrix form [19]. However; as it was in Born Method; this is an ill-posed problem for the Newton Method. So in order to regularize the problem, Tikhonov regularization will be used [19].

$$B\delta v^{(1)} = \left[u_s(x) - F\left(v^{(0)}\right)\right] \Longrightarrow (\alpha I + B^* B)\delta v^{(1)} = B^*\left[u_s(x) - F\left(v^{(0)}\right)\right] \quad \textbf{(3.18)}$$

Now one can take the inverse of the matrix by the same constrains used in section 3.1.1.

$$\delta v^{(1)} = (\alpha I + B^* B)^{-1} B^*\left[u_s(x) - F\left(v^{(0)}\right)\right] \quad \textbf{(3.19)}$$

After $\delta v^{(1)}$ is found ;

$$v^{(1)} = v^{(0)} + \delta v^{(1)} \quad \textbf{(3.20)}$$

is written. $v^{(1)}$ is the new guess for the object function. The same procedure will go on for the same $v^{(1)}$. After n iterations , $v^{(n)}$ will be:

$$v^{(n)} = v^{(n-1)} + \delta v^{(n)} \quad \textbf{(3.21)}$$

3.2.2 Multi-source Effect on Newton Method

As well as in Born Method; it is expected for Newton Method better results from the same reasons mentioned above. The formulation of Newton based on multi-source will be changed in terms of source based function. Therefore; our matrixes will be larger for the same unknowns.

$$F\left(v^{(0)}\right) = k_2^2 \int_D G(x;y)\, v^{(0)}(y) u^{(0)}(y,z) dy \;\Rightarrow\; u^{(0)}\left(y^{p'}, z^q\right) = [I - A]^{-1} u_i(y^{p'}, z^q) \quad \textbf{(3.22)}$$

where A is same with the expression in section 3.2.1, $q = 1,2..Q$ source number and $p' = 1,2,...P$ observation points inside D_R region. The approximation for the observers, sources and the center points of cells in D_R is same with Born multi-source.

$$k_2^2 \int_D G(x;y)\, u^{(0)}(y,z) \delta v^{(1)} dy = u_s(x,z) - F\left(v^{(0)}\right) \quad \textbf{(3.23)}$$

In order to reduce that integral equation to the matrix form;

$$B_{tp} = k_2^2 \int_{D_{R_p}} G(x^r; y^p) u^{(0)}(y^p, z^q) dy \quad \text{where} \quad t = (r,q) \quad \textbf{(3.24)}$$

From now on; the same procedure will go on as it was in Newton Method with single source. For regularization process;

$$B\delta v^{(1)} = \left[u_s(x,z) - F\left(v^{(0)}\right)\right] \Longrightarrow (\alpha I + B^* B)\delta v^{(1)} = B^*\left[u_s(x,z) - F\left(v^{(0)}\right)\right] \quad \textbf{(3.25)}$$

$$\delta v^{(1)} = (\alpha I + B^* B)^{-1} B^*\left[u_s(x,z) - F\left(v^{(0)}\right)\right] \quad \textbf{(3.26)}$$

$v^{(n)}$ can be written from equation (3.21).

4. NUMERICAL APPLICATIONS

Some numerical results which test the accuracy, effectiveness and acceptance of the inverse problem methods; Born and Newton Methods are given in this section. It contains wide analysis and comparisons for single and multi source, single and multi objects, the computational cost, the profit of reflection, Born and Newton Methods. The geometries of the problem is based on Figure 1.1; except for some results which will be explained. On the measurement/scattering data for the given geometry; we will try to find the location, physical and geometrical properties of the buried object. In the simulations done, MATLAB programme is used. As mentioned in section 2; for the integrals MATLAB *'quad'* function which is based on adaptive Simpson quadrature is used. This numerical integration method has an 10^{-6} error tolerance. The same limits explained in section 2 are used in the simulations next. The organization of the section is as follows: In 4.1 Born Method's numerical results will be given. It will include single source, multi-source and two objects applications and comparisons. In 4.2 Newton Method's numerical results will be given with respect to single source, multi-source, two objects, the profit of reflection and the computational cost analysis and comparisons.

4.1 Numerical Results for Born Method

Firstly Born Method for a single source is demonstrated. Then we will check multi-source effect's results for the same configuration and compare them.

For the first simulations; we took the data from a rectangulardielectric object which has the side lengths $2m$ x $2m$ and relative dielectric constant and conductivitiy $\varepsilon_{obj} = 2.5$,

$\sigma_{obj} = 5\text{x}10^{-3}$ $(\frac{S}{m})$ respectively. The first medium or upper part is free space. The parameters of the second medium, lower part, are $\varepsilon_2 = 3$, $\sigma_2 = 10^{-3}$ $(\frac{S}{m})$. These parameters are almost same with dry soil. Magnetic permeability of the medium and the dielectric object are same with free space for all simulations. For the present simulation $f = 10\ MHz$. The cell sides are chosen $\frac{\lambda_{obj}}{60} x \frac{\lambda_{obj}}{60}$. These values are chosen according to the constrains mentioned in section 2. The source and the observer points are symmetric with respect to the dielectric object as it will be chosen generally in the simulations. The source, the object, reconstruction domain and observer locations are seen in Figure 4.1. There is one source and 21 observer points. The scaling parameter in Tikhonov Regularization, $\alpha = 10^{-14}$ is chosen. Figure 4.2 is the imaginary part of object function in reconstruction domain for the solution of Born Method for one source. It can be said from the figure that, Born with single source is not very succesful for shape. Also for the true profile; the imaginary part of the object function is about 1.8 so figure is not true for the physical properties of the object where can be seen from colorbar of Figure 4.2 . However it can be suggestive about location with a tolerance. We will try to fix the results by using multiple source which creates some expectation in the sense of the formulation used in section 4.1.2 .

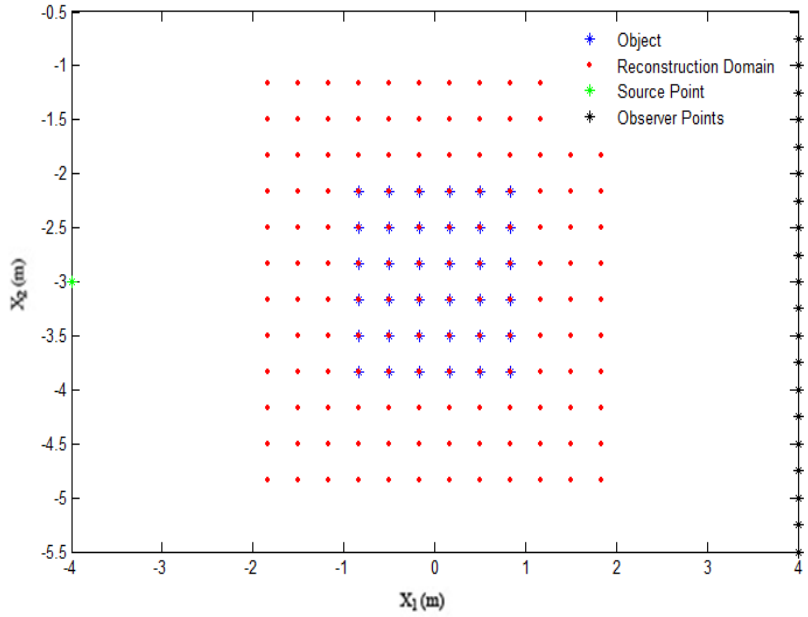

Figure 4.1: The geometry of the forward problem with single source

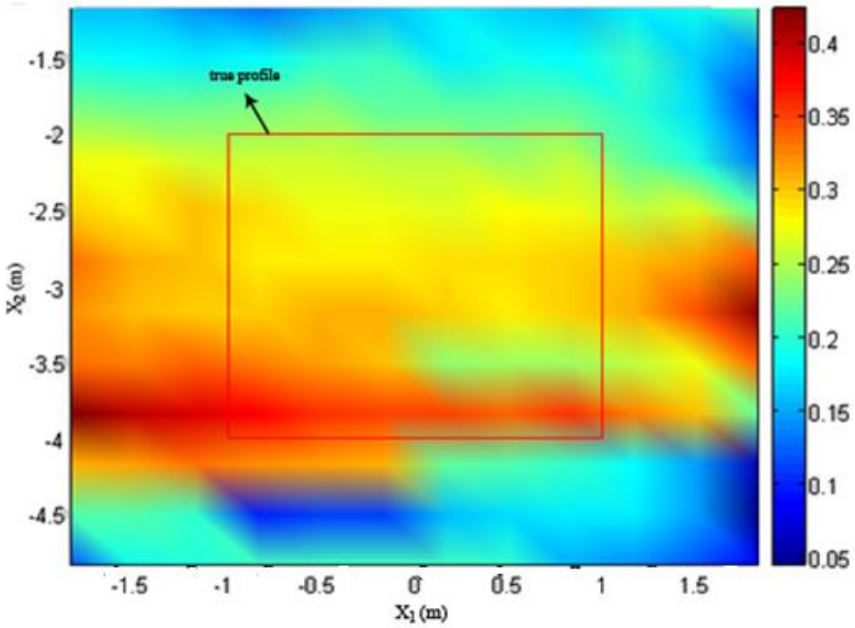

Figure 4.2: The imaginary part of the estimated object's function with Born Method for the given geometry in Figure 4.1

For the simulations of multi-source; we used 5 sources in the same conditions and configuration except for the scaling parameter in Tikhonov Regularization, $\alpha = 10^{-11}$ is chosen. The location of the sources where has a symettry with respect to the object, can be seen in Figure 4.3 .

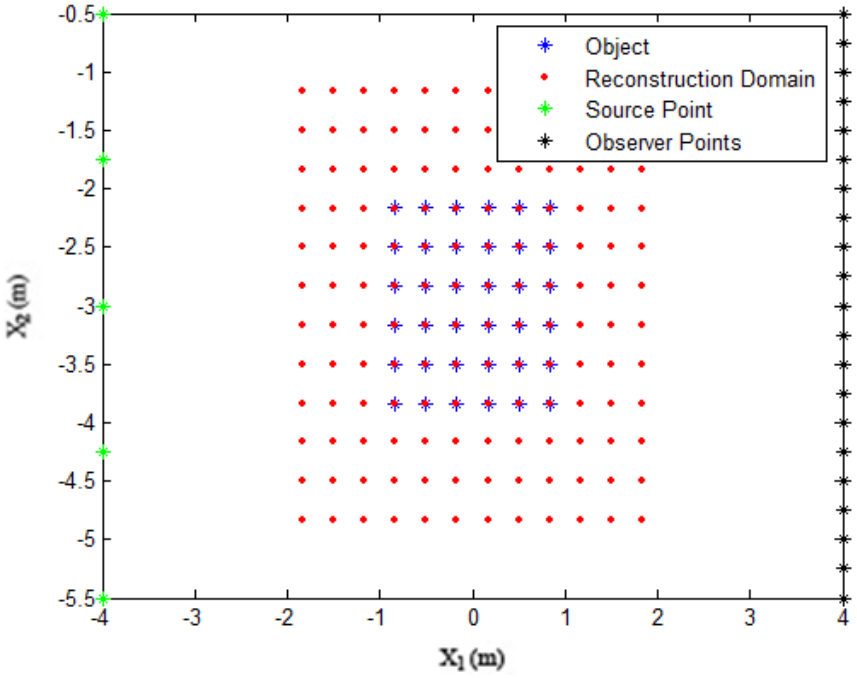

Figure 4.3: The geometry of the forward problem with multiple sources

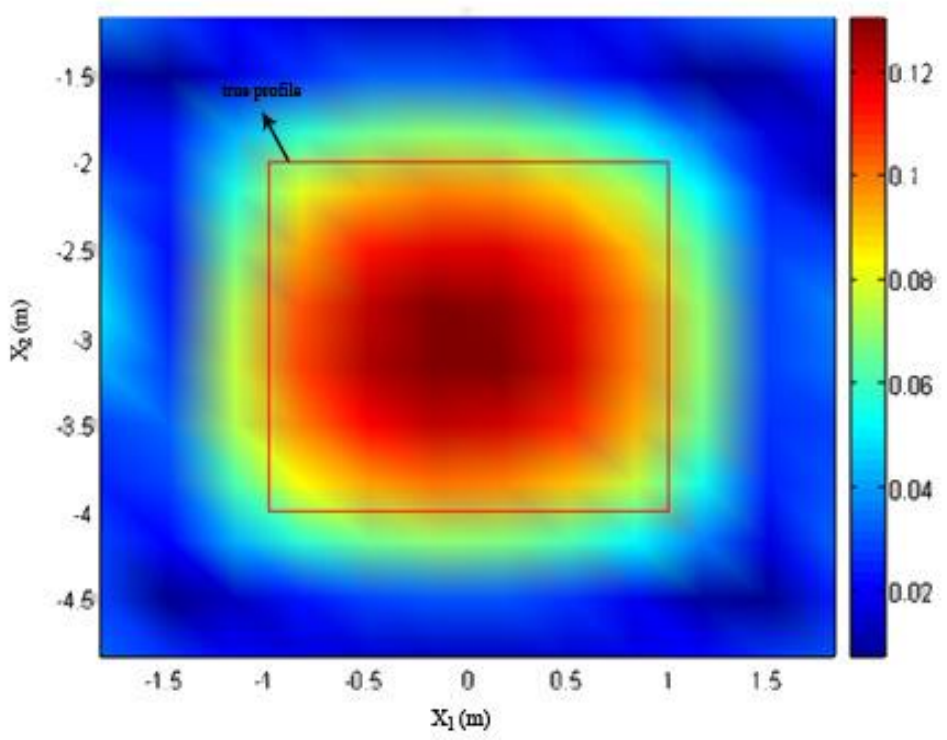

Figure 4.4: The imaginary part of the estimated object function with Born Method for the given geometry in Figure 4.3

Figure 4.4 shows the imaginary part of the estimated object function. It is obvious that multi-source effect brings a serious difference compared to single source. The shape and the location is almost same with the true profile. Multi-source brings a good contrast for the objects buried in a configuration we used. However our estimated object function's imaginary part does not suit the true object's. The imaginary part of the true object's function was 1.8; however the biggest value according to the colorbar for our object is about 0.12; which shows the big difference between them. This may be a disadvantage for Born multi-source inspite of the advantages mentioned. So the multi-source Born gives very good solutions for shape and location of the object; except for the physical properties.

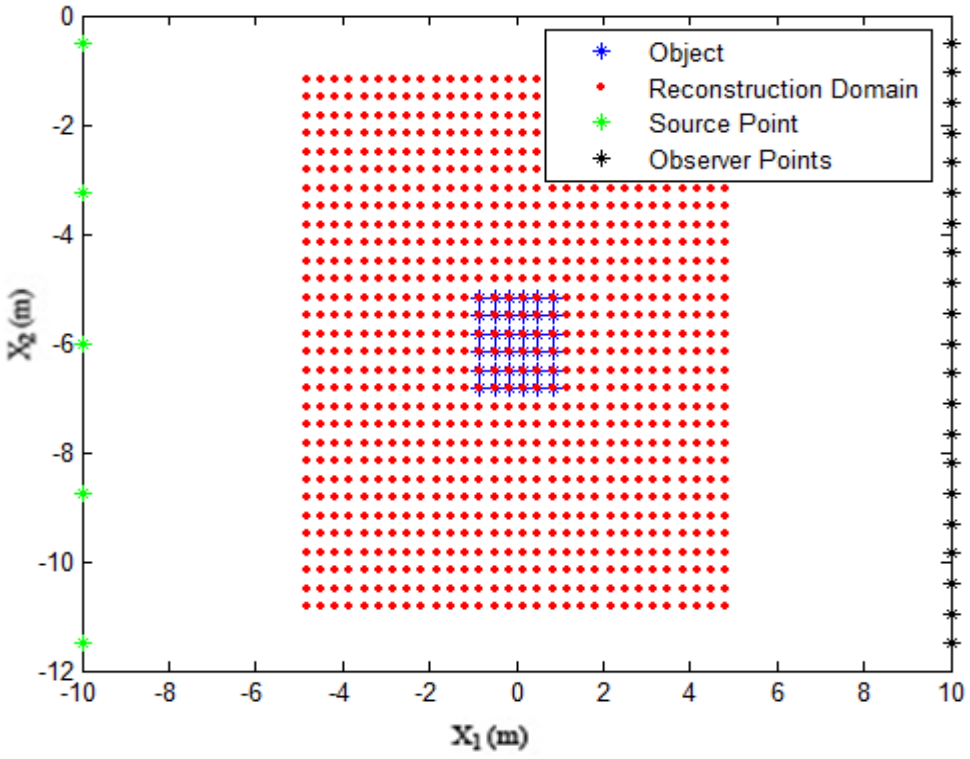

Figure 4.5: The geometry of the forward problem with multiple-source with a bigger reconstruction domain

Figure 4.5 is another geometry to test the Born Method. The source and observer numbers are same with the previous configuration. The object size is also same; but the location of them changed as it can be seen from the figure. The main difference is that the reconstruction domain is bigger than the previous one which means in the inverse problem the sizes of the matrix increased depending on increased unknown cell parameters. The scaling parameter in Tikhonov Regularization, $\alpha = 10^{-12}$ is chosen for the same physical properties of the object. However, for the same source and observer numbers; the contrast of the estimated object to the reconstruction domain compared to

the Figure 4.4 is not reasonable. The result can be seen from Figure 4.6.

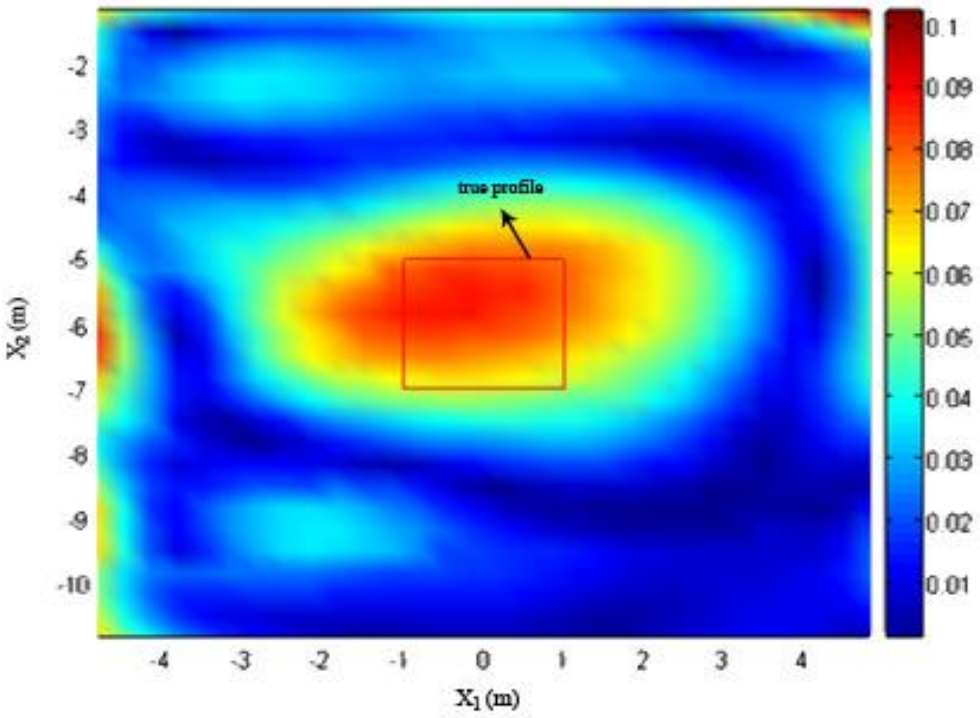

Figure 4.6: The imaginary part of the estimated object function with Born Method for the given geometry in Figure 4.5

As a result of the previous simulation, the complexity of an inverse problem increases; it became harder to solve the problem. Besides; it brings more and more computational cost which is very critical for the solution of these kinds of problems. In order to have more idea about the accuracy and validation limits for Born multi-source, we will increase the complexity by taking the measurement data from two objects in a bigger reconstruction domain than previous example. Figure 4.7 illustrates two objects had a distance at $2\lambda_2$ (according to the parameters of second medium). The parameters of the mediums are same; the dielectric objects which have the same size lengths ($2m$ x $2m$) and relative dielectric constant and conductivitiy of the buried objects are equally $\varepsilon_{obj} = 2$, $\sigma_{obj} = 5\text{x}10^{-3}$ $(\frac{S}{m})$ (the physical properties of charcoal) respectively. $f = 30\ MHz$ is chosen because smaller values than this frequency can not detect two

objects distinctive since the resolution is getting worse while the wavelength increases. For this complex configuration; we should increase the source and observer number for acquring more datas. The source and observer numbers will be 15, 31 respectively. The scaling parameter in Tikhonov Regularization, $\alpha = 10^{-14}$ is chosen. The real part of the estimated object function can be seen from Figure 4.8 . There is a contrast between the objects and the reconstruction domain; however real parts of true profiles object function is -0.18 where the estimated ones are about 0.25. In Figure 4.8, there seems some other shapes, differently from the real objects. The configuration may be hard to solve with Born's method, which gives some ideas about the limits of the method. Whereas it's obvious that Born's Method can give good results for the location and shape but it is not good for the physical properties of the objects. Newton's iterative approach can be a solution for that problem.

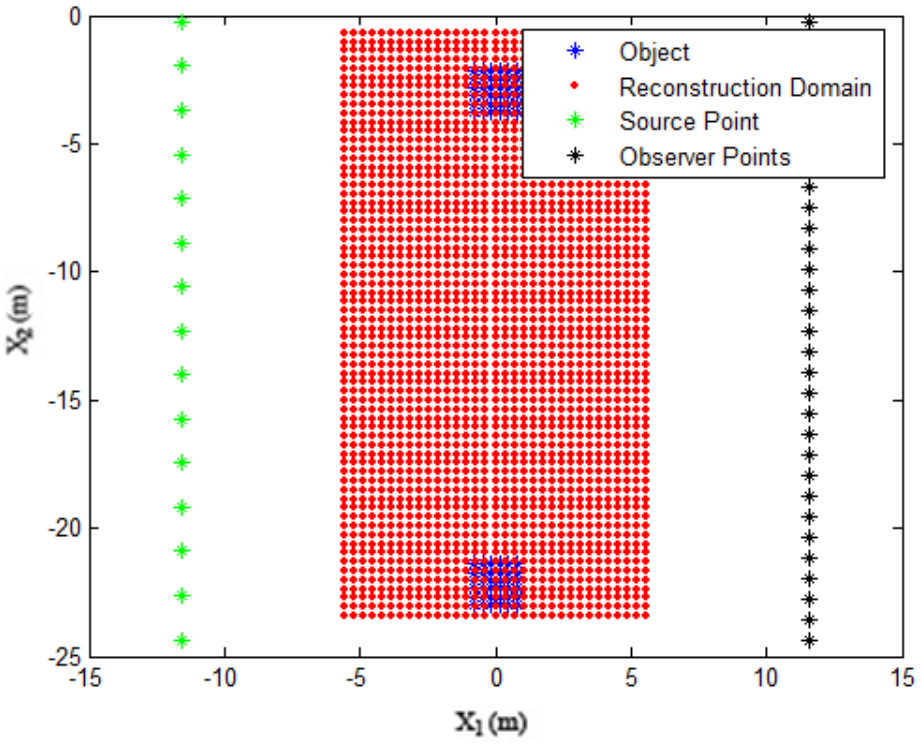

Figure 4.7: The geometry of the forward problem with multiple sources with two objects had a distance $2\lambda_2$

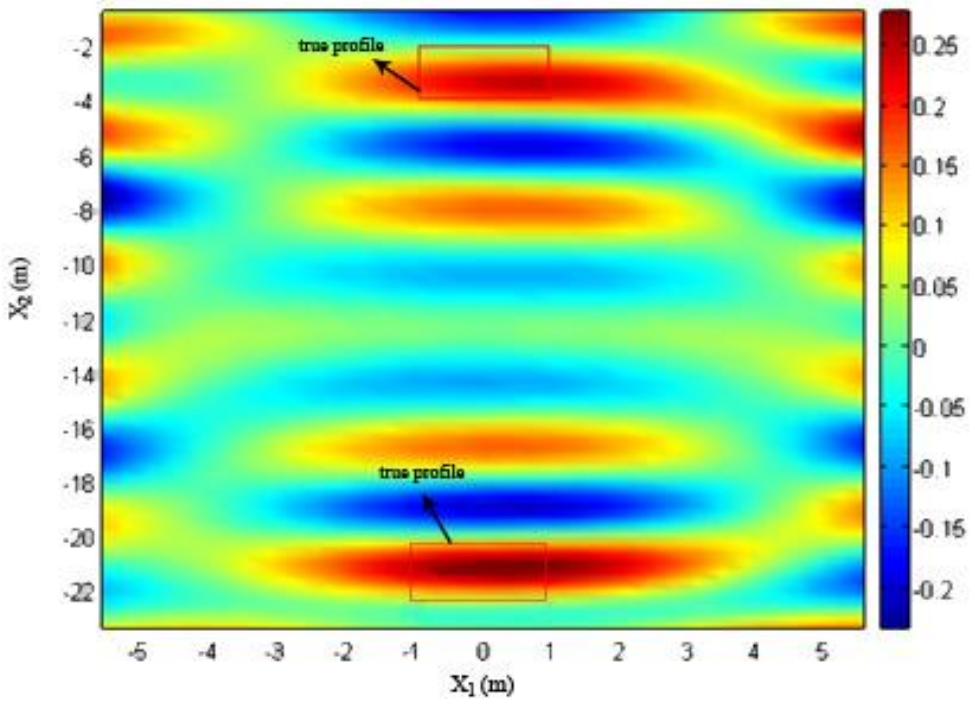

Figure 4.8: The real part of the estimated object function with Born Method for the given geometry in Figure 4.7

4.2 Numerical Results for Newton Method

After simulations for Born; we will present some simulations for the inverse problems based on Newton's Method. The procedure will be almost same; firstly we will apply Newton's Method for single source; then for multi-source and multi objects. Additionally, we will illustrate some simulations to see the profit of the reflection coefficient (equation (2.40)) subject to 2-part medium, then we will finish with some simulations which have a purpose to decrease the computational cost.

The first result is for the single source Newton Method. The parameters of the mediums are same (free space and dry soil); relative dielectric constant and conductivitiy of the object is $\varepsilon_{obj} = 2$, $\sigma_{obj} = 5\text{x}10^{-3}$ $(\frac{S}{m})$ (the physical properties of charcoal) respectively. $f = 10\,MHz$ is chosen. $v^{(0)}$, the initial guess, which is an important

parameter, is chosen as $\varepsilon^{(0)} = 2.5$, $\sigma^{(0)} = 10^{-3}$ $(\frac{S}{m})$ in terms of initial relative dielectric constant and initial conductivity. Iteration number is chosen as 100 manually which is enough to converge; since after 100 iterations there were almost no change on the figure. The scaling parameter in Tikhonov Regularization, $\alpha = 10^{-12}$ is chosen. The same configuration in Figure 4.1 is used.

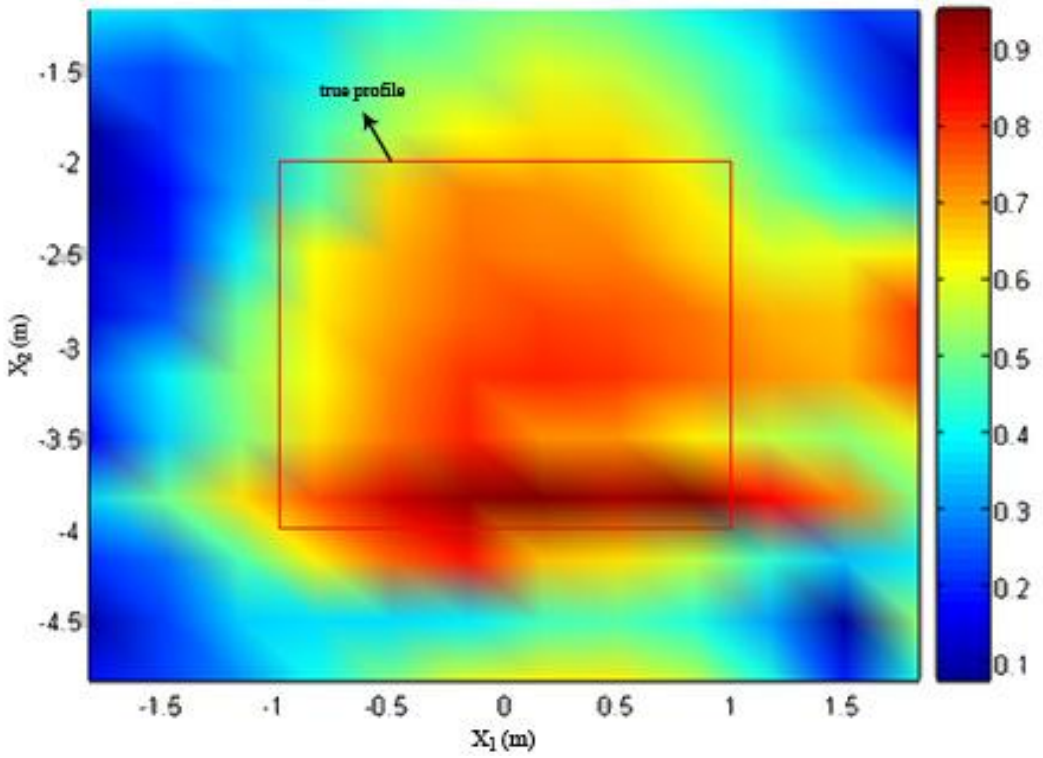

Figure 4.9: The imaginary part of the estimated object function with Newton Method for the given geometry in Figure 4.1

Figure 4.9 is the imaginary part of the object function. Newton Method with the single source cofiguration seems to give better results compared to the Born's Method with single source configuration. For the present simulation, the true profile's object function for imaginary part is 1.8 however estimated one is about 0.8. Whereas it converges better than Born; subject to geometrical and physical properties.

Multi-source should make the solutions better as we proofed it from Born's Method. In these simulations, we used the algorithm explained from equations (3.22) until (3.26). Applying this algorithm for the same configuration in Figure 4.3 will give us chance to compare them with the good results of the Born muliple-source. The parameters of the mediums are same (free space and dry soil); relative dielectric constant and conductivitiy of the object is $\varepsilon_{obj} = 2$, $\sigma_{obj} = 5\text{x}10^{-3}$ $(\frac{S}{m})$ (the physical properties of charcoal) respectively. $f = 10\,MHz$ is chosen. $v^{(0)}$, the initial guess is chosen as $\varepsilon^{(0)} = 2.5$, $\sigma^{(0)} = 10^{-3}$ $(\frac{S}{m})$ in terms of initial relative dielectric constant and initial conductivity. Iteration number is chosen as 100. The initial guess and the iteration number will be taken same for the other simulations unless otherwise stated. The scaling parameter in Tikhonov Regularization, $\alpha = 10^{-8}$ is chosen. The next two figures will be the real and imaginary part of the real object's function respectively. From Figure 4.10 the real part of the estimated object is about 0.7 where our real object's is 0.8, and from Figure 4.11 for the imaginary part 1.7 and 1.8 which are really good convergences.

If we compare Figure 4.4 with Figure 4.11, Born and Newton Methods with multi-source effect are the same from the view of detecting location and shape as inverse algorithms. However, Newton's method is obviuosly better than Born method in estimating the values of the object's function. Newton method suggests better solutions than Born from the aspect the and physical properties of the object.

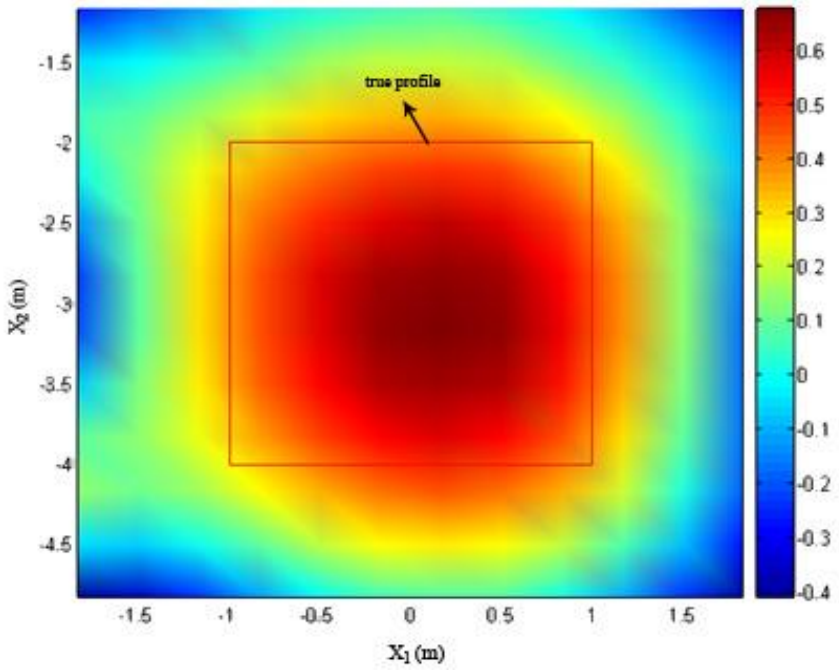

Figure 4.10: The real part of the estimated object function with Newton's Method for the given geometry in Figure 4.3

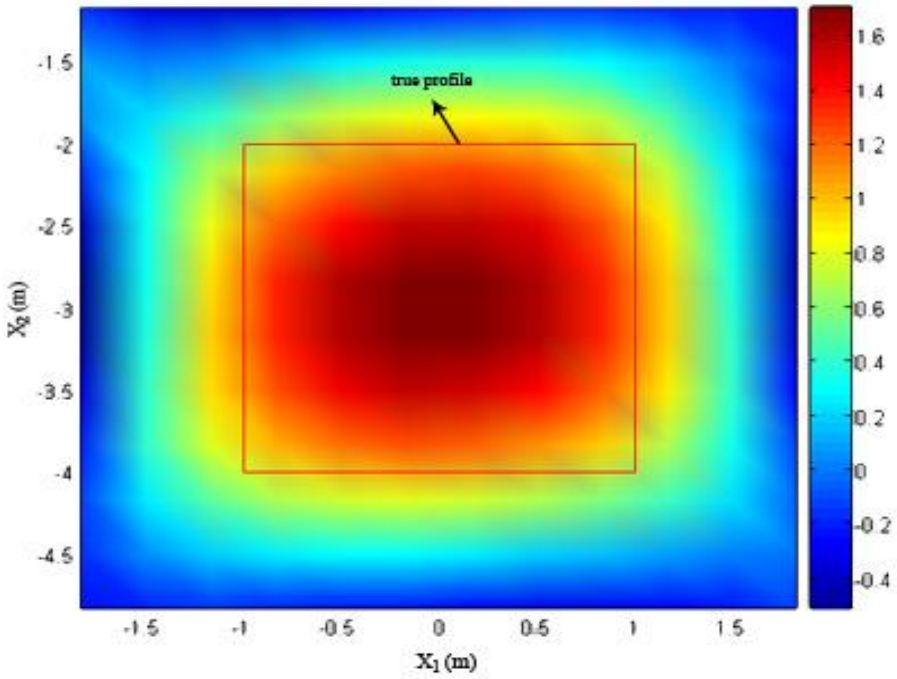

Figure 4.11: The imaginary part of the estimated object function with Newton's Method for the given geometry in Figure 4.3

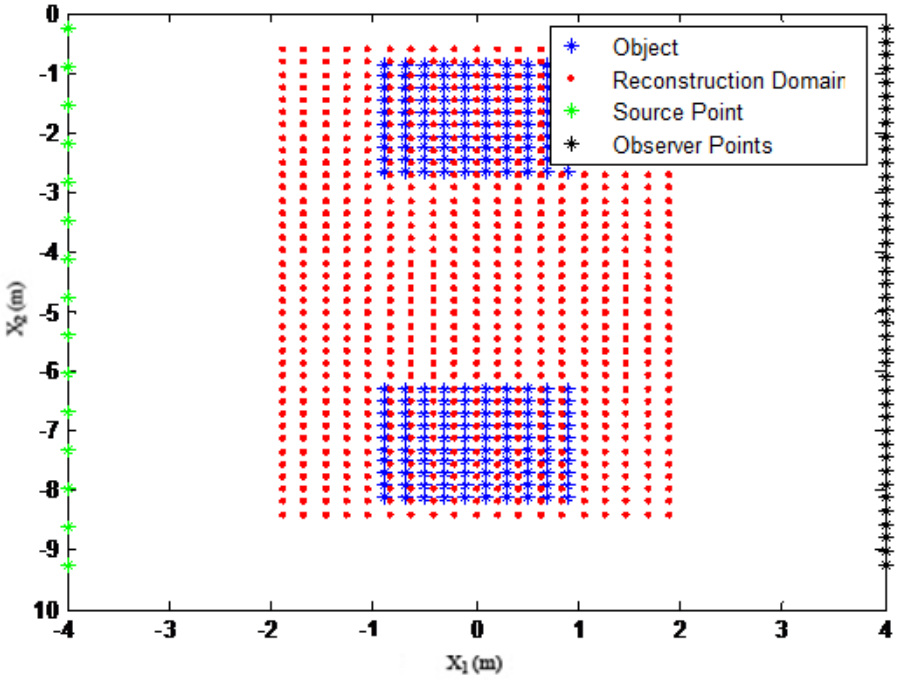

Figure 4.12: The geometry of the forward problem with multiple sources with two objects had a distance λ_2

We will solve the inverse problem using the measurement data of the configuration in Figure 4.12. We know that Newton's method using multi-source gives good results; but we want to test the limits and accuracy of it by increasing the complexity of the configuration. The objects are equal by geometry and physical properties. For the first simulations; we took the data from a dielectric object which has the size lengths ($2m$ x $2m$) and relative dielectric constant and conductivitiy of the objects are same as charcoal. The mediums are the same as all simulations. For the present simulation $f = 50\ MHz$. The cell sides are chosen $\frac{\lambda_{obj}}{20}$ x $\frac{\lambda_{obj}}{20}$. The scaling parameter in Tikhonov Regularization, $\alpha = 10^{-4}$ is chosen.The initial guess and iteration number are same with the previous simulation.

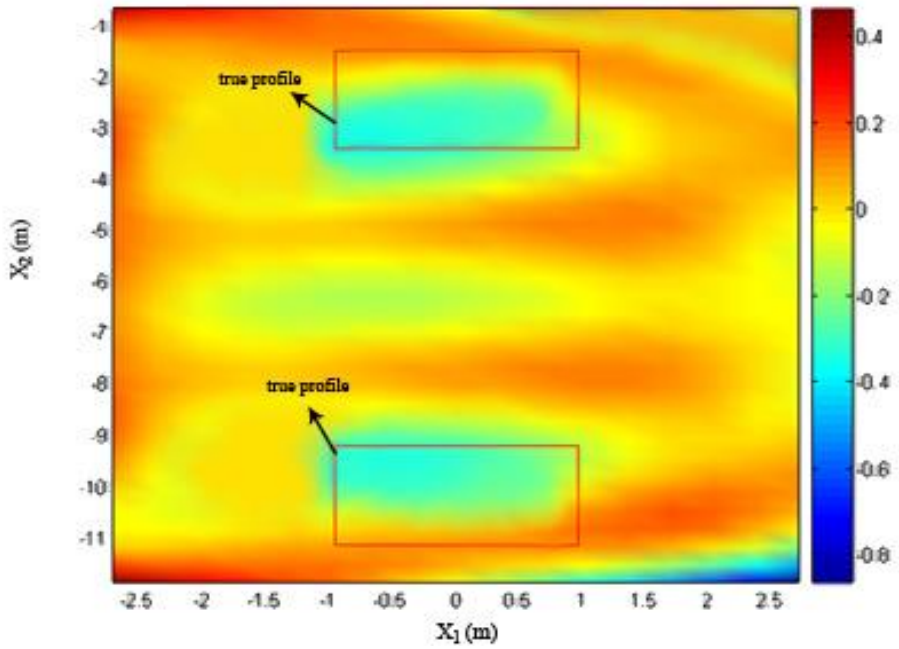

Figure 4.13: The real part of the estimated object function with Newton Method for the given geometry in Figure 4.12

The real part of the true object's function is -0.27 which is close to our estimated result. And also the imaginary part of the true object's function is 0.51 which is close to the value of the estimated object. They are shown in Figure 4.13 and 4.14 respectively. These results are also better than Born's Method in the solution of two objects configuration if the contrasts of the Figure 4.8 and 4.14 are compared. Now we will test the Newton's method for two different objects in terms of size and physical properties. Figure 4.15 is the configuration for the measurement data; the observer and source numbers, locations with the objects sizes and reconstruction domain as well. The frequency for the present simulation is $f = 50\,MHz$. The cell sides are chosen $\frac{\lambda_{obj}}{20}$ x $\frac{\lambda_{obj}}{20}$. The scaling parameter in Tikhonov Regularization, $\alpha = 10^{-7}$ is chosen. The other parameters for Newton Method's algoritm is same with the previous simulation.

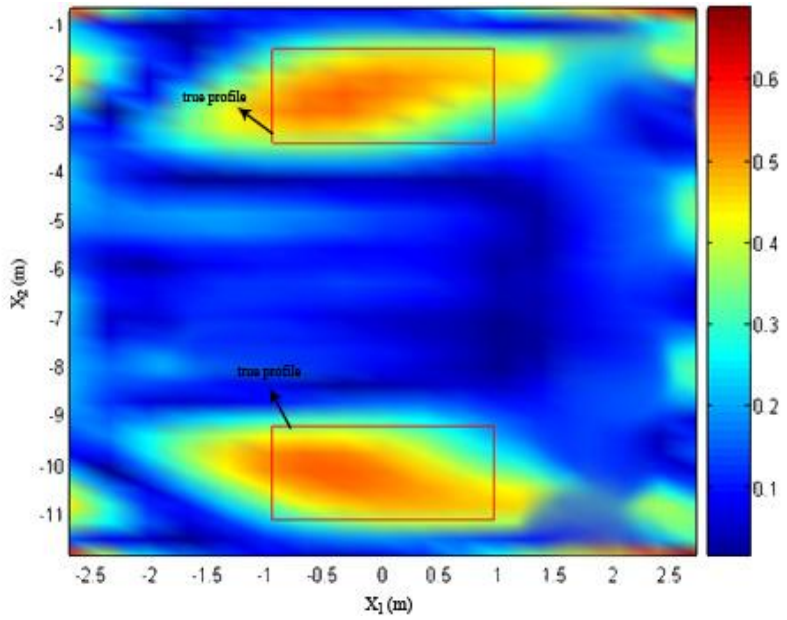

Figure 4.14: The imaginary part of the estimated object function with Newton Method for the given geometry in Figure 4.12

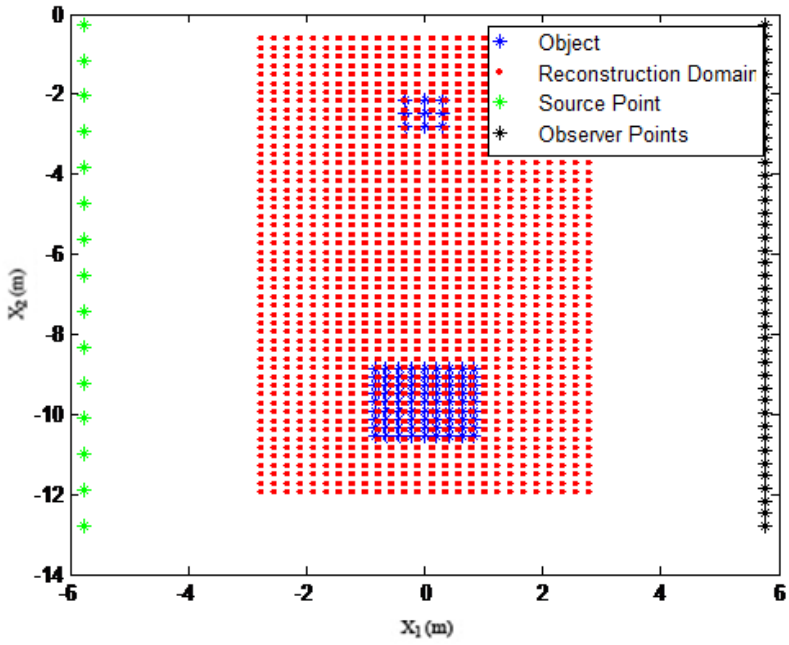

Figure 4.15: The geometry of the forward problem with multiple sources with two objects have different properties

Figure 4.16, the real part of the true object function, and Figure 4.17, the imaginary part of the true object's function, are the simulation results for two different objects have sizes ($1m$ x $1m$) and ($2m$ x $2m$) respectively. The real and imaginary part of the smaller object -0.27 and 0.51, the real and imaginary part of the other one is 0.6 and 0.7 respectively.

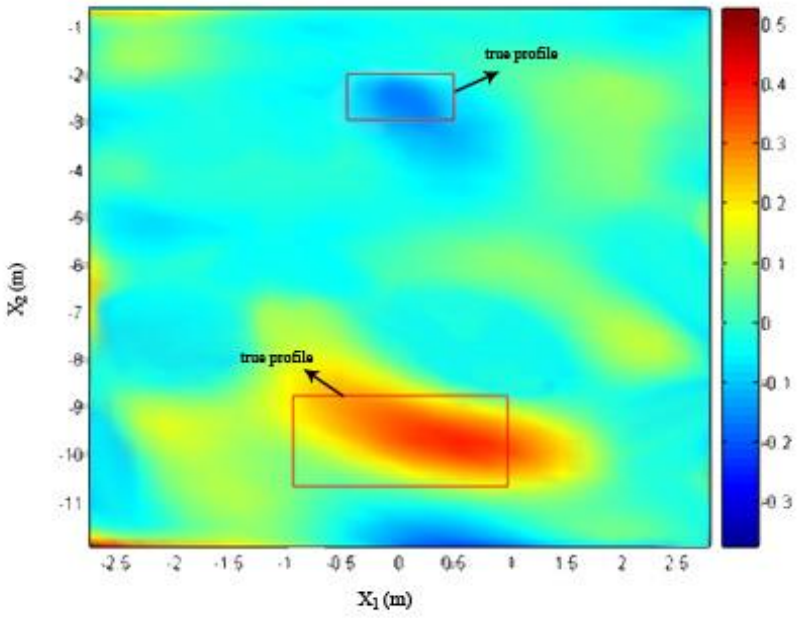

Figure 4.16: The real part of the estimated object function with Newton's Method for the given geometry in Figure 4.15

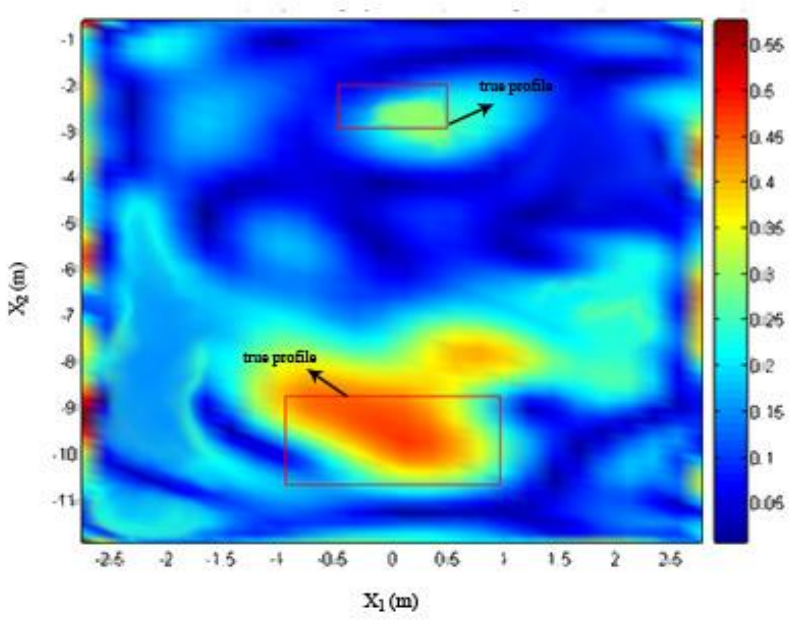

Figure 4.17: The imaginary part of the estimated object function with Newton's Method for the given geometry in Figure 4.15

So as it can be seen from the figures above; the estimated values are close to the values of the objects. This type of location for the objects, give good results for the given geometry. However, it is known from the simulations done in this thesis that this source and observer configuration subject to the locations of them, does not give good solutions for the objects alongside. In this situation one of the objects close to the source are disappeared; because of the shadowing. But we did not give any example about the configuration mentioned.

The starting point of the thesis was that; two part mediums can be a profit if the geometry of the problem is like in Figure 1.1. Because the reflected wave will behave as a second source; and changes the results as the multiple source effect did (the contribution of equation (2.40)). There is a simulation about this comparison below. The configuration used in Figure 4.1 will be used for this comparison. We know how Newton's method behaves for a configuration like this from Figure 4.9. Figure 4.9 is the condition when the reflection exists. So if we imagine as everywhere dry soil or second

medium, that means there will be no reflection, in other words our imaginary source coming from reflection is ignored. We will choose the same parameters for all parameters with the structure in Figure 4.8 except for the reflection. We will just ignore first medium. Here is the result for no reflection in Figure 4.18.

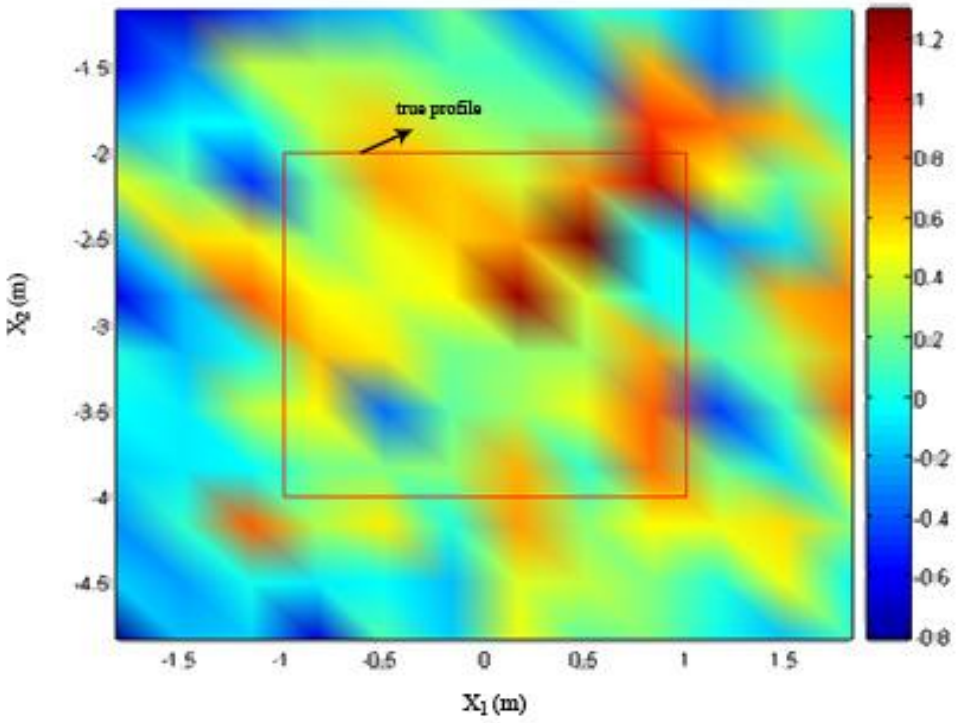

Figure 4.18: The imaginary part of the estimated object function with Newton's Method for the given geometry in Figure 4.1 without the reflection parameter

If we compare the result of Figure 4.18 with Figure 4.9 it is obvious that Figure 4.9 means more than Figure 4.18 in terms of imaging buried objects. By the way convergence to the result in Figure 4.18 by the scaling parameter α is really hard compared to the 4.8. That means reflection brings an imaginary but maybe a weak source to the configuration of Figure 4.18. However the reconstruction algorithm used for the structure of Figure 4.18 is much better about the computational cost. Because, in the two part medium configuration, a numerical integral coming from equation (2.26)

and (2.40) is evaluated for huge matrixes. We ignore it in that simulation by means of ignoring reflection. That situation becomes suggestive for us to test the computational cost.

Regardless, the measurement data won't change in the practical applications. So from the aspect of the computational cost, we can decrease it just for the reconstruction process by ignoring the reflected wave. Because the contribution of reflection (equation (2.40)) can be accepted smaller compared to the transmitted one (equation (2.39)). So that the forward problem will be solved in terms of reflection; but in the reconstruction process, reflection will be ignored to reduce computational cost. We tested it with multi-source, and we used the configuration for taking the measurement scattered data from Figure 4.3. Their test results are given in Figure 4.10 and Figure 4.11. When we ignore the reflection for the reconstruction process for the same parameters used in the solution of Figure 4.10 and 4.11; the results are below.

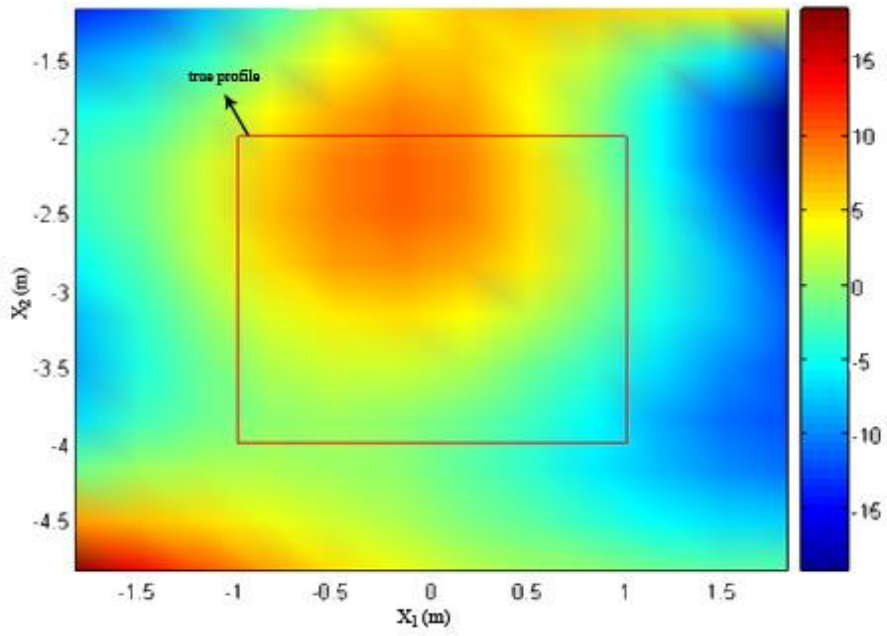

Figure 4.19: The real part of the estimated object function with Newton's Method for the given geometry in Figure 4.1 ignoring the reflection parameter in reconstruction process

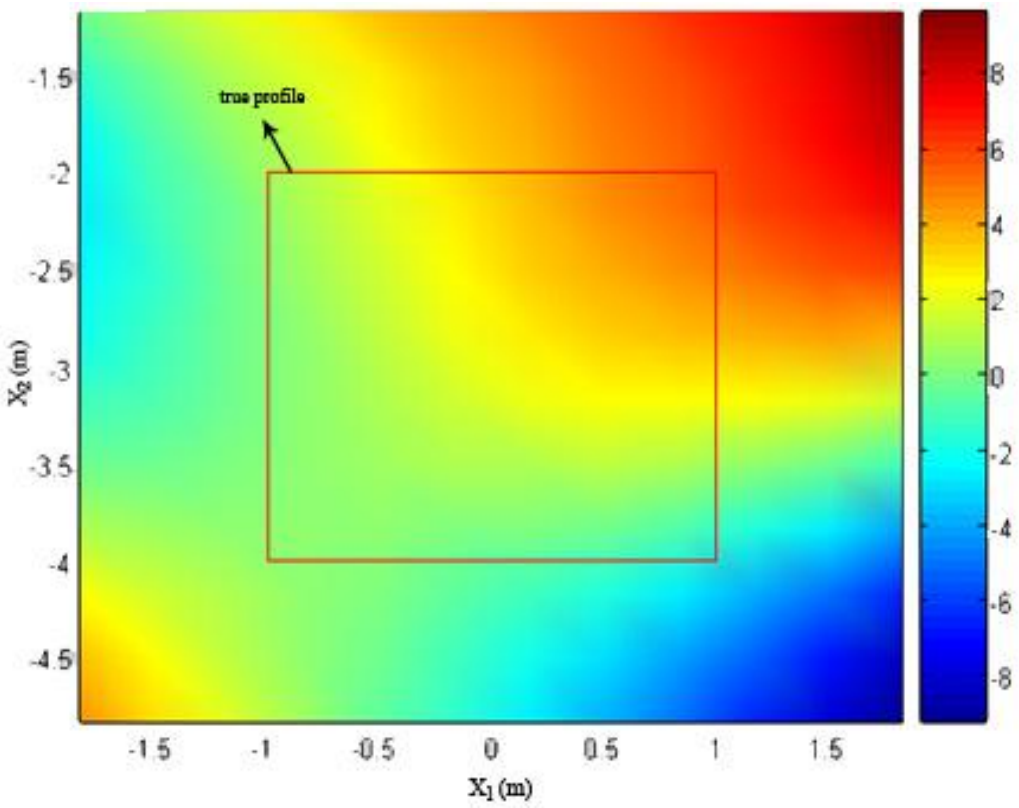

Figure 4.20: The imaginary part of the estimated object function with Newton's Method for the given geometry in Figure 4.1 ignoring the reflection coefficient in reconstruction process

As it can be seen from the results; it can not converge more than seen in the figures. So for the measurement data that has additionally reflection part, the reconstruction process can not be solved without thinking it. In other words, the costly part in computations can not be ignored for a configuration given in Figure 4.3.

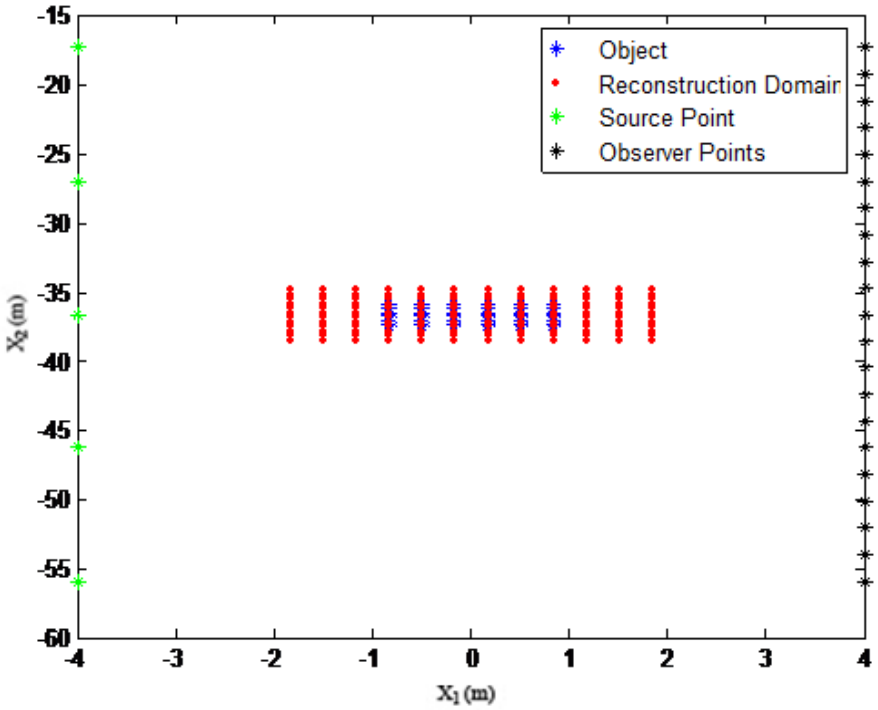

Figure 4.21: The geometry of the forward problem with multiple sources for a single object deeper than λ_2 from the surface

As a result of Figure 4.20 and 4.21, it can be said that the reflection coefficient makes an important contribution, however it is known as weak compared to the coefficient in equation 2.39. Moreover, it is also known that if the distance between the surface and the object increases, reflected wave will be weaker. So this gave another idea that what if the object is deeper as Figure 4.21 than the configuration in Figure 4.3 . We get the measurement data according to the forward problem of the present configuration. The physical properties and the sizes of the objects are still same.

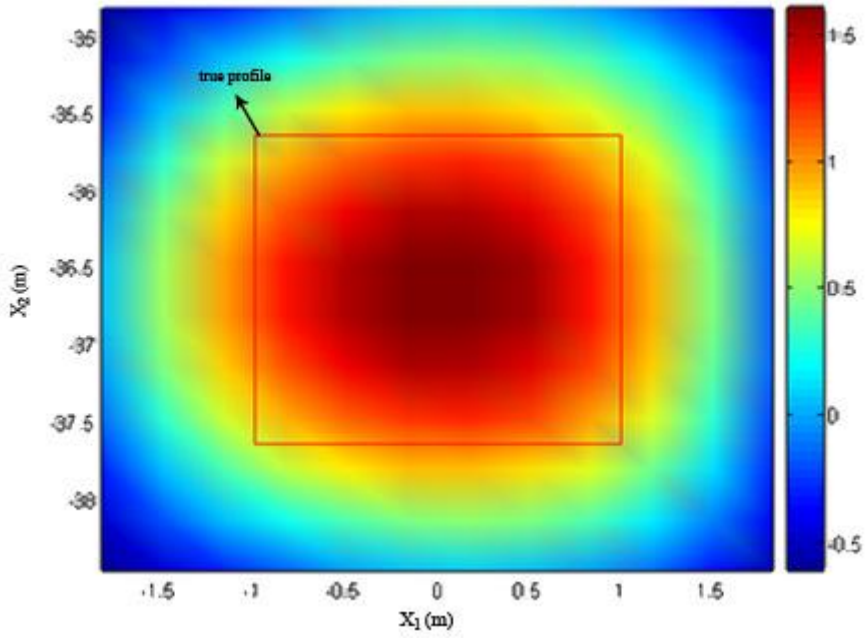

Figure 4.22: The imaginary part of the estimated object function with Newton's Method for the given geometry in Figure 4.21 including the reflection coefficient in reconstruction process

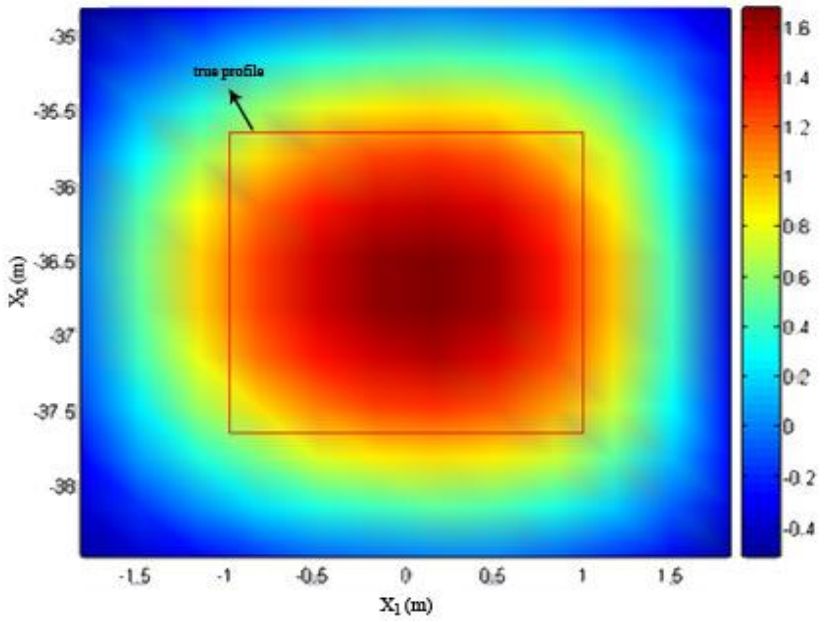

Figure 4.23: The imaginary part of the estimated object function with Newton's Method for the given geometry in Figure 4.21 ignoring the reflection in reconstruction process

The only difference is that, the object is deeper more than 30 m. compared to the configuration in Figure 4.3. Figure 4.22 and 4.23 are almost same. But the algorithm used in Figure 4.22 has a computational cost much more bigger because of the evaluation of the numerical integral coming from the reflection coefficient (equation (2.40)) than the algorithm used in Figure 4.23. What makes this result important that for the configurations which objects are deeper, the reflected wave (equation (2.26) and equation (2.4)) can be ignored to reduce the computational cost.

All results will be concluded in section 5, conclusion part.

5. CONCLUSIONS

In this thesis, 2-D buried objects in two part space with a planarly interface is based on the method called borehole in geoscience. The geometry of the problem is mentioned in section 1. In order to solve inverse problem, firstly the forward problem must be solved to create the measurement/scattered field data. Although solution of the forward problem is not main for this thesis, the solution of it makes valueable contributions to the inverse probelm; as choosing the bounds in the numerical integration methods or choosing the cell size's of the objects for the MoM. Since that validation limits determine the accuracy and stability of the methods used in the solution of the inverse problem. For inverse problem, Born and Newton Method are used.

Born relies on using the incident field instead of total field in Fredholm integral equations. Thus, the object function can be evaluated from the measurement data. Born Method is applicable for the geometry and physical properties used in this work because of the weak scattering. Therefore one can ignore scattered field, and use the incident field instead of the total field. However, the results of the Born Method for single source are not succesful from the view of the shape and physical properties of the object. But when the number of the sources increases that gives really good results in terms of the shape and the location. This is an important consequence of the thesis. However for the physical properties like the object function; Born Method does not work. In order to handle this, Newton Method can be applied.

Newton Method is an effective iterative approach which is more complex than Born Method. It brings better solutions. The multiple source has the same effect for the Newton Method. By that positive effect of multisource; the Newton' s algorithm gives really good results in the way of physical properties, object function. Also it gives the

exact location and shape for the single object configuration. This is an important consequence of the thesis, too. Newton gives better solutions for more complex configurations such as two objects in a big reconstruction domain. Here is an important consequence; for two objects; the frequency should be chosen bigger than single object in the way of the resolution but under the constraints of cell size and computational cost.

One of the consequences can be explained according to the numerical applications done: The profit of the reflection. The planarly interface for two part space brings important advantage because of the geometry of the problem. The reflection parameter comes additionally different from one part space. This reflection parameter can be imagined as an additional source symmetrical to the actual source on the planar interface. Therefore it brings beter results compared to the one part space configurations. One part space configurations can not converge in the sense of α scaling parameter in Tikhonov Regularization. α the scaling parameter is chosen as trial and error because it is not in the concept of the thesis. Whereas it is very important to choose α, which can affect the solution directly. Another consequence can be explained in terms of computational cost. Pursuant to the measurement data, the reconstruction process can have less computational cost for Newton Method if the object is deeper than a distance equal to the wavelength of the second medium (dry soil). Since at a distance mentioned, the reflected term of the reconstruction process can be ignored. It means the numerical integrations are ignored which is really worse from the aspect of the computational cost.

Finally, for the further work other inverse algorithms such as Born iterative and distorted Born may be tried to compare the results with those of Newton. It can be worked on computational cost on these types of problems. It can also be interesting to work on the best choice of α the scaling parameter in Tikhonov Regularization.

REFERENCES

[1] Url-1 < *http://www.numathics.com* >, accessed at 01.05.2010.

[2] Url-2 < *http://en.wikipedia.org/*>, accessed at 01.05.2010.

[3] Devaney, A. J., 1984: Geophysical diffraction tomography, *IEEE Trans. Geosci. Remote Sensing*, Vol. **GE-22**, no. 1, pp. 3-13.

[4] Harris, J. M., 1987: Diffraction tomography with arrays ofdiscrete sources and receivers, *IEEE Trans. Geosci. Remote Sensing*, Vol. **GE-25**, pp. 448-455.

[5] Richmond, J.A., 1965: Scattering by a dielectric cylinder of arbitrary crosssection shape, *IEEE Trans. on Antennas and Prop*, Vol. **13 (3)**, pp.334-341.

[6] Tanaka, M., Takenakata, T., and Tabuchi, Y., 1993: Electromagnetic Imaging Of Scattering Objects in Cross-Borehole Measurements, *IGARSS'93: Better Understanding Of Earth Envinronment*, Vol. **I-IV**, pp. 1900-1902.

[7] Devaney, A. J., and Beylkin, G., 1984: Diffraction tomography using arbitrary transmitter and receiver surfaces, *Ultrasonic Imaging*, Vol. **6**, pp. 181-193.

[8] Witten, A. J., and Long, E., 1988: Geophysical imaging with arbitrary source illumination, *IEEE Trans. Geosci. Remote Sens.*, Vol. **26**, pp. 409.

[9] Chaturvedi, P., and Plumb, R. G., 1995: Electromagnetic imaging of underground targets using constrained optimization, *IEEE Trans. Geosci. Remote Sensing*, Vol. **33**, pp. 551 - 561.

[10] Bao, G., and Li, P., 2007: Inverse medium scattering problem in near-field optics, *J. Comp. Math.*, **25**, pp. 252–265.

[11] Cui, T. J., Chew, W. C., and Hong, W., 2004: New approximate formulations for EM scattering by dielectric objects, *IEEE Trans. Antennas Propag.*, Vol. **52**, pp. 684. 27.

[12] Bozza, G., Estatico, C., Pastorino, M., and Randazzo., A., 2007: "Application of an Inexact-Newton method within the second-order Born approximation to buried objects", *IEEE Geosci. Remote Sens. Lett.*, Vol. **4**, pp. 51.

[13] Balanis, C. A., 1989: *Advanced Engineering Electromagnetics*, Wiley, Arizona.

[14] Chew, W. C., 1995: *Waves and fields in inhomogeneous media*, IEEE Press, NJ.

[15] Ishimaru, A., 1991: *Electromagnetic Wave Propagation, Radiation and Scattering*, Prentice Hall, New Jersey.

[16] Felsen, LB. and Marcuvitz, N., 1973: *Radiation and Scattering of Waves*, Printice Hall, New Jersey.

[17] Harrington, R.F., 1968: *Field Computation by Moment Methods*, Macmillan, Newyork

[18] Cui, T. J., Chew, W. C., and Hong, W., 2004: New approximate formulations for EM scattering by dielectric objects, *IEEE Trans. Antennas Propag.*, Vol. **52**, pp. 684.

[19] Rieder, A., 1999: On the regularization of nonlinear ill-posed problems via inexact Newton iterations, *Inv. Probl.*, Vol. **15**, no. 1, pp. 309–327.

[20] Yapar, A., 2006: A regularized Newton method for one-dimensional profile inversion of a lossy cylinder, *AEU-International Journal of Electronics and Communications*, Vol. **60 (8)**, pp. 590-595.

[21] Hohage, T., and Schorman. C., 1998: A newton-type method for a transmission problem in inverse scattering, *Inverse Problems*, **14**, pp. 1207–27.

CURRICULUM VITA

Candidate's full name: Ulaş ADIYAN

Place and date of birth: Van, 30.11.1983

Permanent Address: Doğuş University, Dep. of Electronic and Communication Eng.

Universities and Colleges attended: İTÜ (İstanbul Technical University)